

Journal Pre-proof

Lessons from the COVID-19 air pollution decrease in Spain: Now what?

Xavier Querol, Jordi Massagué, Andrés Alastuey, Teresa Moreno, Gotzon Gangoit, Enrique Mantilla, José Jaime Duéguez, Miguel Escudero, Eliseo Monfort, Carlos Pérez García-Pando, Hervé Petetin, Oriol Jorba, Víctor Vázquez, Jesús de la Rosa, Alberto Campos, Marta Muñoz, Silvia Monge, María Hervás, Rebeca Javato, María J. Cornide



PII: S0048-9697(21)01448-0

DOI: <https://doi.org/10.1016/j.scitotenv.2021.146380>

Reference: STOTEN 146380

To appear in: *Science of the Total Environment*

Received date: 4 February 2021

Accepted date: 5 March 2021

Please cite this article as: X. Querol, J. Massagué, A. Alastuey, et al., Lessons from the COVID-19 air pollution decrease in Spain: Now what?, *Science of the Total Environment* (2021), <https://doi.org/10.1016/j.scitotenv.2021.146380>

This is a PDF file of an article that has undergone enhancements after acceptance, such as the addition of a cover page and metadata, and formatting for readability, but it is not yet the definitive version of record. This version will undergo additional copyediting, typesetting and review before it is published in its final form, but we are providing this version to give early visibility of the article. Please note that, during the production process, errors may be discovered which could affect the content, and all legal disclaimers that apply to the journal pertain.

© 2021 Published by Elsevier.

Lessons from the COVID-19 air pollution decrease in Spain: Now what?

Xavier Querol¹, Jordi Massagué^{1,2}, Andrés Alastuey¹, Teresa Moreno¹, Gotzon Gangoiti³, Enrique Mantilla⁴, José Jaime Duéguez⁴, Miguel Escudero⁵, Eliseo Monfort⁶, Carlos Pérez García-Pando^{7,8}, Hervé Petetin⁷, Oriol Jorba⁷, Víctor Vázquez^{9,10}, Jesús de la Rosa¹¹, Alberto Campos¹², Marta Muñoz¹², Silvia Monge¹², María Hervás¹², Rebeca Javato¹², María J. Cornide¹²

¹*Institute of Environmental Assessment and Water Research, IDAEA-CSIC, Barcelona, 08034, Spain*

²*Department of Mining, Industrial and ICT Engineering, Universitat Politècnica de Catalunya - BarcelonaTech (UPC), Manresa, 08242, Spain*

³*Department of Chemical and Environmental Engineering, University of Basque Country, Leioa, 48940, Spain*

⁴*Centro de Estudios Ambientales del Mediterráneo, CEAM, València, 46080, Spain*

⁵*Centro Universitario de la Defensa, Academia General Militar, Zaragoza, 50090, Spain*

⁶*Instituto de Tecnología Cerámica ITC-UJI, Castelló, 12006, Spain*

⁷*Barcelona Supercomputing Center, BSC-CNS, Barcelona, 08034, Spain*

⁸*ICREA, Catalan Institution for Research and Advanced Studies, Barcelona, 08010, Spain*

⁹*Department of Ecology, Faculty of Sciences, University of Málaga, 29011, Málaga, Spain*

¹⁰*Department of Research and Development, Cocosphere Environmental Analysis, 29120, Málaga, Spain.*

¹¹*Department of Geology, University of Huelva, Huelva, 21811. Unidad de Investigación Asociada a IDAEA-CSIC, Spain*

¹²*D.G. Calidad y Evaluación Ambiental del Ministerio de Transición Ecológica y Reto demográfico, Madrid, 28071, Spain*

ABSTRACT

We offer an overview of the COVID-19-driven air quality changes across 11 metropolises in Spain with the focus on lessons learned on how continuing abating pollution. Traffic flow decreased by up to 80% during the lockdown and remained relatively low during the full relaxation (June and July). After the lockdown a significant shift from public transport to private vehicles (+21% in Barcelona) persisted due to fear of infection, which need to be reverted as soon as possible. NO₂ levels fell below 50% of the WHO annual air quality guidelines (WHOAGs) but PM_{2.5} were reduced less than expected due to its lower contributions from traffic, increased contributions from agricultural and domestic biomass burning, or large secondary aerosol contributions. Even during the lockdown, the annual PM_{2.5} WHOAG was exceeded in cities within the NE and E regions with high NH₃ emissions from farming and agriculture. Decreases in PM₁₀ levels were greater than in PM_{2.5} due to reduced emissions from road dust, vehicle wear, and construction/demolition activities. Averaged O₃ daily maximum 8-hours (8hDM) experienced a generalized decrease in the rural receptor sites in the relaxation (June-July) with -20% reduced mobility. For urban areas O₃ 8hDM responses were heterogeneous, with increases or decreases depending on the period and location. Thus, after cancelling out the effect of meteorology, 5 out of 11 cities experienced O₃ decreases during the lockdown, while the remaining 6 either did not experience relevant reductions or increased. During the relaxation period and coinciding with the growing O₃ season (June-July), most cities experienced decreases. However, the O₃ WHOAG was still exceeded during the lockdown and full relaxation periods in several cities. For secondary pollutants such as O₃, further chemical and dispersion modeling along with source apportionment techniques to identify major precursor reduction targets are required to evaluate the O₃ abatement potential.

Keywords: air quality, tropospheric ozone, air quality policy, pollution abatement

1. INTRODUCTION

The COVID-19 pandemic—caused by the global spread of the coronavirus SARS-CoV-2—has created an unprecedented human health impact, with infections and deaths exceeding 100 million and 2 million, respectively, as of 20/01/2020 (John Hopkins University, 2021). To reduce the spread of SARS-CoV-2, lockdown measures have been implemented worldwide with varied timing and severity according to the onset of the epidemiological crisis and the evolution of infections. Shifts in human mobility patterns resulting from the enforced confinement/lockdown associated with the COVID-19 pandemic (Chakraborty & Maity, 2020) offer a unique opportunity to identify the effects of human presence on urban and background air quality and advance our understanding of air pollution. On average across Europe, emission reductions were estimated to be about -33 % for NO_x , -8 % for NMVOCs, -7 % for SO_x and -7 % for $\text{PM}_{2.5}$ during the most severe lockdown period (23 March to 26 April 2020), with road transport being the largest contributor to total reduction (85 % or more) except for SO_x (Guevara et al., 2021). In countries where the lockdown restrictions were more severe such as in Italy, France or Spain, reductions were even larger, reaching about -50 % (NO_x), -14 % (NMVOCs), -12 % (SO_x) and -15 % ($\text{PM}_{2.5}$). As a result, many studies related to the impact of COVID-19-related emission reductions on air quality have been published in recent months (e.g., Baldasano, 2020; Bawens et al., 2020; Collivignarelli et al., 2020; Petetin et al., 2020; Tobías et al., 2020; Huang et al., 2020; Le et al., 2020, Chen et al., 2020; Silver et al., 2020; Nakada et al., 2020; Barré et al., 2020; Huang et al., 2020; Le et al., 2020, Chen et al., 2020; Silver et al., 2020; Nakada et al., 2020, Le Quéré et al., 2020, Liu et al., 2020, Shi et al., 2021). Such studies encompass a range of pollutants that include gases such as NO_2 , O_3 , and CO_2 as well as atmospheric particulate matter finer than 2.5 and 10 μm ($\text{PM}_{2.5}$ and PM_{10} , respectively). In this context, we offer a comprehensive overview of the impact of the COVID-19 crisis across 11 metropolitan areas of Spain to extract lessons for the future implementation of cost-effective air quality improvement policies in the coming post-pandemic society.

2. METHODOLOGY

2.1. Metropolitan areas and lockdown stages

2.1.1. Selected cities

We considered eight of the ten most populated metropolitan areas in Spain (Madrid, MAD; Barcelona, BCN; València, VAL; Sevilla, SEV; Málaga, MAL; Bilbao, BIL; Zaragoza, ZAR; Murcia, MUR) and three less populated areas (A Coruña, COR; Valladolid, VLD; Badajoz, BAD) to ensure good spatial coverage of the mainland territory (Table 1 and Figure 1).

The climates of these cities range from hot summer semi-arid Mediterranean (BCN, VAL, SEV, and MAL) to the milder and moist Atlantic coastal conditions in N Spain (BIL and COR), to the more continental Iberian microclimates inland (MAD, BAD, ZAR, MUR, and VLD).

Regarding industrial activity, INE (2020) provides indicators to assess industrial development in the Spanish autonomous regions (i.e., total turnover, number of businesses, investment in tangible assets, and number of workers). In 2018, Catalonia (where BCN plays a primary role),

Andalucía (with Huelva, not studied here, and SEV), Madrid (MAD), València (with hotspots in Castelló, not studied here, and VAL), and the Basque Country (especially the BIL area) were the highest-ranking autonomous regions for the aforementioned indicators.

MAD and BCN have the highest number of vehicles (Table 1), followed by VAL, SEV, MAL, and MUR, while COR, BIL, ZAR, BAD, and VLD have the lowest number (DGT, 2020). In terms of vehicle density (vehicles/km²), MAD and BCN are also at the top of the list, while BIL is in third position.

Airports are present near all the selected cities. According to AENA (2020), in terms of passengers, the MAD and BCN airports stood out with 22.4 and 19.1% of all passengers in 2019, respectively, followed by MAL, VAL, SEV, VLD, and BAD with 7.2, 3.1, 2.7, 0.09, and 0.03%, respectively.

Important commercial and passenger harbors are present in BCN, VAL, MAL, BIL, COR, and SEV. Data from Jan-Sep 2020 indicate that BCN, VAL, and BIL harbors are the most active with 5,047, 4,440, and 1,695 ships, respectively, from January to September 2020, with lower levels of activity in the remaining harbors (ranging from 572 to 811 ships) (Puertos del Estado, 2020). Cruising activity is very important in BCN (199,842 passengers in the first three months of 2020), MAL, and VAL (40,172 and 26,286 passengers, respectively). For fishing vessels, COR is the most active harbor (24,652 ships during the aforementioned period).

Agriculture- and farming-related atmospheric pollutant emissions are widespread in Spain. Agricultural burns often occur around all of the selected cities, especially MUR, SEV, VLD, VAL, COR, BIL, and ZAR, and in autumn, winter, and spring. Furthermore, the autonomous regions of Aragón, Catalonia, and Murcia (where ZAR, BCN, and MUR are located, respectively) are atmospheric NH₃ hotspots due to intensive emissions from farming and the agricultural use of organic fertilizers (Van Damme et al., 2018).

2.1.2. Stages of the COVID-19 lockdown and subsequent relaxation

In Europe, lockdowns started in Italy on 09/03/2020 and one week later in Spain (on 16/03/2020). In the present study, we distinguish between periods and sub-periods associated with the different confinement stages of each city (Figure 2). We considered 1) a reference pre-pandemic period between 14/02/2020 and 15/03/2020, 2) a lockdown period between 16/03/2020 and 24/05/2020, and 3) a full relaxation period (hereafter referred to as “full relaxation”) between 24/05/2020 and 31/07/2020. We considered the lockdown period to comprise 1) a partial lockdown period (hereafter referred to as “partial lockdown-1”) between 16/03/2020 and 29/03/2020, when the “stay home” order was recommended, 2) a full lockdown period (hereafter referred to as “full lockdown”) between 30/03/2020 and 13/04/2020, 3) another partial lockdown period when the “stay home” order was mandatory and non-essential industries were shut down (hereafter referred to as “partial lockdown-2”) between 14/04/2020 and 01/05/2020, and 4) the first stage of the so-called relaxation period (stage 0 and stage 1). Indeed, the relaxation of measures was performed in five stages starting on 02/05/2020. However, since most of the lockdown restrictions remained in place during stages 0 and 1, both stages remained within the lockdown period for this study. The start and end dates of stages 1, 2, and 3 differed in each region according to the local evolution of the pandemic (see Figure 2 for further details). This was followed by what we refer to as the full relaxation period (stages 2, 3, and 4).

The lockdown imposed drastic restrictions on human activities, including road traffic, industry, and urban mobility. Data on activity in the different cities across various sectors were collected from the historical geo-localization of cell phones with activated GPS and were obtained from Google LLC (2020). A summary of this data is presented in Figure 3a and detailed information is provided in Table S1. Retail and recreational mobility was drastically reduced by 85 (MUR) to 89% (BIL) during the lockdown, and by 80 (MUR) to 93% (BIL, MAL, and VLD) during the full lockdown when compared to pre-lockdown. During full relaxation, mobility remained reduced by between 25 (MAL) and 38% (MAD). Thus, the mobility restrictions similarly affected all of the studied metropolitan areas during the partial and full lockdown (only 3–4% maximum differences). However, the varied timing of full relaxation stages generated larger differences among cities (13–54% relative difference) during full relaxation. The number of circulating vehicles decreased by only 4% more than workplace mobility during weekdays in BCN (Figure 3b) (-77 and -74% from 16/03/2020 to 09/04/2020, respectively). However, there was a 21% increase during the full relaxation period (-18 and -39% averages for June and July, respectively). This suggests that a substantial proportion of commuters may have avoided public transportation and used private cars due to fear of SARS-CoV-2 infection. This shift in transport mode is potentially relevant to the design of future measures to improve urban air quality.

Figure 3b shows that the consumption of natural gas by industry was only slightly reduced compared to the 2016–2019 average, with only a 1% decrease in April and May. However, important differences were observed in harbors (Puertos del Estado, 2020). For example, the number of ships in the harbor of BIL did not decrease substantially—and even increased—during the lockdown when compared to the harbors of SEV, COR, and BCN, where traffic fell by 20–35% in March and April (Figure 3c). While a decrease in the number of ships was recorded in VAL, the numbers recovered in May and decreased again in June. During the lockdown, the number of fishing vessels increased substantially (+200%) in COR, decreased by 50% in BCN, and were highly varied in VAL (Figure 3d). Moreover, the number of cruises was reduced to 0 from May in BCN and VAL, and from April in COR.

2.2. Air quality data, monitoring sites and data treatment

The present work relied on daily average concentrations of air pollutants (NO, NO₂, CO, SO₂, NH₃, O₃, PM₁₀, and PM_{2.5}) calculated from hourly measurements taken at 131 air quality monitoring (AQM) stations in mainland Spain operated by local and regional monitoring networks and compiled by the Spanish Ministry of Environment between 2015 and 2020 (Figure 1). In each metropolitan area, we considered two categories of AQM stations: 1) metropolitan, to assess most pollutants within conurbations and 2) receptors, which are located in areas outside of the cities but affected by metropolitan plumes. Therefore, this information can be used to assess O₃ formation downwind.

For each AQM station and pollutant, we determined the daily concentrations (i.e., daily maximum 8-hour averages (8hDM) for O₃) based on hourly measurements for days with at least 75% of hourly data available, as suggested by the Directive 2008/50/CE (EC, 2008). We then calculated average and period (pre-pandemic, lockdown, and full relaxation) concentrations for each pollutant for each year between 2015 and 2020 while considering only the periods with at least 75% data availability.

To assess changes in concentrations during the lockdown, we only considered the pollutants and periods with 1) at least 3 years of valid data for the 2015–2019 period and 2) valid data in 2020 (i.e., if the 2020 lockdown NO_2 data from a certain AQM station was missing or the availability was $<70\%$, NO_2 data from that station during the equivalent lockdown periods within 2015–2019 were ignored). We also averaged the concentrations for urban areas (metropolitan) and those for the receptor areas.

Spain is frequently affected by N African dust outbreaks (NAF), which can influence PM levels (Querol et al., 2019a and b). These NAF contributions were considered when evaluating the impact of the lockdown on PM levels. The daily NAF contributions to PM levels (both NAF- PM_{10} and NAF- $\text{PM}_{2.5}$) were calculated between 14/02 and 31/07 for the years 2015 to 2020 following a modified version of the method from Escudero et al. (2007), which is accepted by the European Commission (EC, 2011). Thus, our calculations were performed for the PM_{10} and $\text{PM}_{2.5}$ levels as well as for the $\text{PM}_{10\text{sub}}$ and $\text{PM}_{2.5\text{sub}}$ levels (i.e., after subtracting the NAF contributions).

2.3. TROPOMI-NO2

For NO_2 tropospheric observations, we used data from the high-resolution nadir-viewing satellite sensor, the Tropospheric Monitoring Instrument (TROPOMI), onboard the Sentinel-5 Precursor (Veefkind et al., 2012). We processed TROPOMI global daily gridded data at $0.05^\circ \times 0.05^\circ$, which were derived from the offline operational product (van Geffen et al., 2019) via a script in Google Earth Engine (Gorelick et al., 2017). TROPOMI has an overpass local time of 13:30 h GMT and provides a resolution of $5.5 \times 3.5 \text{ km}^2$. We used data with a quality assurance value >0.75 . To retrieve tropospheric NO_2 , we selected pixels from overpass areas for each metropolitan area of interest. Each area is defined by a convex polygon whose vertices are the locations of the most external AQM sites in each metropolitan area, buffered by 6.5 km (a distance equal to the hypotenuse of a right triangle whose legs are 5.5 and 3.5 km in length).

2.4. Meteorological analysis

Meteorology is a key driving factor for pollutant levels. For example, intense winds bring good venting periods in pollution-affected regions and precipitation effectively cleans the atmosphere by washing or raining out many pollutants. Conversely, low wind intensities and planetary boundary layer heights and/or local and mesoscale wind re-circulations under stable anticyclonic conditions give rise to the accumulation of pollutants and pollution episodes. In the case of secondary species such as O_3 , the activation of photochemical reactions and efficient transport mechanisms for precursor emissions from upwind regions ideally occurs under anticyclonic conditions (i.e., the absence of cloud cover, high solar radiation, and more frequent warm temperatures).

Wind, precipitation, cloud cover, temperature, and pressure distribution anomalies during the pandemic period with respect to the previous five-year (2015–2019) averages were used to gain insights into the role of the meteorology on the observed concentration changes in addition to the direct impact of the emission reductions. Free troposphere fields (700 hPa winds and the topography of the 500 hPa pressure surface) were also included in the analysis to search for general circulation anomalies associated with the prevalence of meridional/zonal winds and African dust outbreaks, among others. We used hourly ERA-5 (ECMWF Reanalysis 5th Generation Description, from European Centre for Medium-Range Weather Forecasts)

reanalysis data (Hersbach et al., 2018), and the Grid Analysis and Display System for data processing and the representation (Doty & Kinter, 1995) of anomalies. Additional information was obtained from the 6-hourly historical archive from the National Centers for Environmental Prediction-Climate Forecast System Reanalysis represented in Wetterzentrale (<http://www.wetterzentrale.de/>; last accessed: 14 November 2020).

2.5. Meteorology-normalized changes in pollutant concentrations

In addition to anomalies in pollutant concentrations during the pandemic with respect to the previous five-year averages, we also estimated the changes in pollutant concentrations solely due to lockdown-induced emission reductions by canceling out the effect of meteorological variability using a meteorology-normalization technique. We used a machine learning (ML)-based weather normalization approach previously used to estimate reductions in surface NO_2 over Spain (Petetin et al., 2020) and Europe (Barré et al., 2020) during the initial weeks of lockdown. Here, we briefly introduce this methodology; however, a complete description and validation can be found in Petetin et al. (2020). This approach consists of training gradient boosting machine models to predict the relationships between pollutant concentrations and a set of input features including ERA5 meteorological parameters (i.e., daily mean 2 m temperature, minimum and maximum 2 m temperature, surface wind speed, normalized 10 m zonal and meridian wind speed components, surface pressure, total cloud cover, net solar radiation at the surface, downward solar radiation at the surface, downward UV radiation at the surface, and boundary layer height) and other time variables (i.e., date index, Julian date, day of the week). Here, this methodology is applied to NO_2 , O_3 , and $\text{PM}_{2.5}$ concentrations. For each pollutant and surface station, specific ML models were trained and tuned over 2017–2019, tested over 2020 before the lockdown (01/01/2020–14/03/2020), and ultimately used during the lockdown and full relaxation periods. This method estimated the business-as-usual (BAU) pollutant concentrations that would have been expected in the absence of COVID-19-related mobility restrictions. The changes in concentrations due to COVID-19 lockdown were then deduced by comparing the estimated BAU concentrations with the observed concentrations.

The overall statistical results are shown in Table S2 for both training and testing datasets. Statistics include the mean bias (MB), normalized mean bias (nMB), root mean square error (RMSE), normalized root mean square error (nRMSE), Pearson's correlation coefficient (r), and the total number of points (N). The performance of the ML models was found to depend on the pollutant considered. For the testing dataset, the best performance was obtained for NO_2 and O_3 (nMB of 6 and 9%, nRMSE of 29 and 24%, r of 0.89 and 0.82, respectively). Comparatively, the bias obtained for $\text{PM}_{2.5}$ sub and bulk $\text{PM}_{2.5}$ were slightly lower (around -3%); however, the nRMSE and PCC (abscissa) deteriorated to approximately 49% and 0.70, respectively. Considering the higher complexity of PM variability compared to NO_2 and O_3 , this result was expected. Since these statistical results were computed over the entire set of stations, lower performance can be encountered for specific individual stations. Overall, the statistical results obtained here are considered reasonably good for estimating reliable BAU pollutant concentrations during the lockdown and full relaxation periods.

Annexes 1 to 3 from the supplementary material show the meteorology-normalized changes in concentrations for each monitoring station and pollutant.

3. RESULTS AND DISCUSSION

3.1. Meteorological patterns during the study period and comparison with 2015–2019

The estimated anomalies of the most relevant meteorological variables are presented in Figure 4, where the periods (i.e., pre-pandemic, lockdown, and full relaxation) are shown in three columns.

The pre-pandemic period was characterized by an intense zonal flow over Iberia. On average, a high-pressure anomaly was centered over N Africa/S Iberia (see the contour lines of the 500 hPa surface in Figure 4a3). This induced higher than usual wind velocities over the entire region (well-marked over the Bay of Biscay) after the location of a polar front close to that latitude. Simultaneously, positive temperature anomalies, with lower than average precipitation and cloudiness, were observed (Figures 4a1–3).

The lockdown was characterized by positive pressure anomalies in the N of Iberia and negative pressure anomalies over the SW of the peninsula (Figures 4b1). The dry continental E winds brought a warm and dry anomalous meteorology to N Iberia, while the low-pressure anomaly to the SW is the footprint of a more frequent development of large Rossby waves or the evolution of isolated low pressures torn off from the region of the polar front and moving to the S of the peninsula and N Africa. These conditions often bring cloudy skies and precipitation to this region (Figures 4b2–3) and can also cause desert dust outbreaks (Gkikas et al., 2015). The described pressure and wind anomalies were compatible with a preferred meridional circulation during the period with prevailing southeasterlies in the free troposphere. The largest positive precipitation anomaly was observed in E Iberia (Figure 4b3), corresponding to a relatively cold region associated with wet E winds over the W Mediterranean, moving toward the low-pressure anomaly to the SW of Iberia. During the final days of the lockdown (19–30/05/2020), the weather of the region changed to a summer type mode (at the surface, the Azores High widely covers the W Mediterranean and an African upper-level ridge extends from N Africa to Iberia) compatible with O_3 accumulation episodes (Querol et al., 2018; Escudero et al., 2019).

The full relaxation (June and July 2020) began with a reversed pressure anomaly distribution in June with respect to the lockdown period, generalized anomalous low temperatures, and high rainfall levels. Negative anomalies of the 500 hPa topography, a cooler mid-troposphere, and NW wind anomalies in the free troposphere were also observed. An exception to the intense ventilation conditions was identified on the E Iberian coast, which remained under anomalous weak winds. The observed meteorology is consistent with an abnormal prevalence of meridional circulations with prevailing northwesterlies in June, resulting from the development of upper-level troughs running N-to-S or the transit of isolated lows crossing the Bay of Biscay into Iberia. Thereafter, June presented an unusual scarcity of typical summer scenarios of the O_3 accumulation mode. The intense low-pressure—as well as precipitation and wind— anomalies in June were compensated for during the entire June–July period (Figures 4c1–3). This resulted in closer-to-average values in the SW regions of Iberia, with warmer temperatures and clear skies (Figure 4c2). Conversely, the NE region did not evolve to more typical values (Figures 4c1–3) and experienced positive rainfall, negative temperature anomalies, and abnormally cloudy skies that persisted throughout July. These relatively cool and wet conditions in July were associated with the development of an upper-level trough,

which crossed continental W-C Europe to the W Mediterranean and lasted for a relatively long period (13–19/07/2020). The W and SW regions of Iberia were kept out of the influence of this unstable meteorology. In summary, the full relaxation and a period of O₃ maximization in Spain (Querol et al., 2016, 2017, 2018) presented favorable meteorology for less frequent and/or shorter ozone episodes.

3.2. Changes in the concentrations of pollutants

3.2.1. NO₂ and NO

NO₂ in the atmosphere largely originates from anthropogenic sources involving high-temperature processes. Data from emission inventories (EEA, 2019) reveal that the main NO_x source in EU-28 cities is road transport (39%), followed by energy production (26%) and domestic sources (14%). The proximity of road traffic enhances the contribution of this source to NO₂ urban background levels. For example, the main sources of NO_x emissions in BCN during 2013 were industry (15%), road transport (37%), and the harbor (52%); however, their contributions to NO_x urban background ambient levels were 2, 60, and 8%, respectively (BCC, 2016). In MAD, industry and road transport accounted for 15% and 47% of the NO_x emissions in 2016, respectively; however, they contributed <1 and 73% of the ambient NO₂ contributions when only local sources are considered and <1 and 53.4% of the bulk ambient urban background concentrations, respectively (UPM, 2017).

Mean NO₂ levels during the pre-pandemic period reached 31 to 37 µg/m³ in BCN, MUR, and MAD, 20 to 26 µg/m³ in BIL, MAL, SEV, VAL, VLD, and ZAR, and only 9 and 10 µg/m³ in BAD and COR. On average, during that month, the European annual limit value of 40 µg/m³ (which coincides with the annual WHO's AQ Guideline, WHOAQG) was only exceeded in traffic (TR) sites of BCN, MUR and MAD. During the lockdown, NO₂ levels decreased to 8–16 µg/m³ in most cities, except for BAD (3 µg/m³) with the highest levels occurring in MUR, BCN, BIL, ZAR, and BIL. Low levels persisted during the full relaxation (7 to 19 µg/m³ across most cities and 5 µg/m³ in BAD).

The decreases in NO₂ throughout the lockdown relative to the same period during 2015–2019 (Figure 5a and Table 2) reached 69% for VAL, 50–56% for VLD, BAD, MAL, BCN, SEV, and MAD, and 39–48% for CCN, MUP, BIL, and ZAR. After applying the meteorological normalization, these reductions were slightly lower (Figure 5b and Table 2), reaching 50–61% in SEV, MAL, BAD, MAD, and VAL and 42–49% for the remaining areas, with the exception of COR (reduction of 34%).

Barré et al. (2020) found a relationship between stricter lockdowns and greater reductions in NO₂ across European cities, with average reductions obtained with TROPOMI NO₂ tropospheric columns and surface stations of 23 and 43%, respectively, between 16/03/2020 and 30/04/2020. The range of reductions across the six Spanish cities included in Barré et al. (2020) was likely wider—from 15 (BIL) to 70% (VAL)—due to the lockdown period being shorter than the one considered here.

Marked reductions during the full relaxation relative to the 2015–2019 average were still evident, reaching 35–43% in SEV, BCN, MAD, VAL, and VLD, and 15–29% in the other cities (Figure 5a and Table 2). In this case, the meteorological normalization yielded smaller reductions likely due to the very wet June 2020, i.e., from 22 (BIL, VLD, VAL, and MAL) to 31%

(BCN) for most cities, excluding the 10 to 18% observed for COR, BAD, MUR and ZAR (Figure 5b and Table 2).

Due to the dramatic reduction in traffic flows during the lockdown (up to 80% during the full lockdown, Figure 6), urban background (UB) and TR sites registered greater reductions (averages of 51 and 49% without and with meteorological normalization, respectively) compared to industrial (IND) and receptor sites (RUR) (43 and 37%, respectively) (Table 2).

In BCN and MAD, (Figure 6a), traffic flow in working days was reduced by 64 and 63% during the lockdown period, with a maximum of 80% during the full lockdown in both cities. During the full relaxation, traffic in BCN and MAD was still reduced by 22 and 34% in June and by 17 and 27% in June-July, respectively, which was likely due to reduced road traffic, industry activity, and harbor operations (in BCN).

However, during lockdown, the proportion of urban freight distribution vehicles increased when compared to the pre-pandemic period. In BCN (Figure 6b), this proportion reached 21 and 14% during the lockdown and full relaxation periods, respectively, while the pre-pandemic proportion was 12%. Most of these vehicles are diesel and generally old, thus emitting more PM_{2.5} and NO_x. Also, by cross-correlating the daily reduction of traffic with NO₂ levels for BCN (Figure 7), we estimated that with a stable fleet composition, a 25 to 30% reduction in traffic on working days is required to avoid exceeding the EU annual NO₂ limit (40 µg/m³) in the two traffic AQM stations where that standard is usually exceeded.

At the regional scale, TROPOMI tropospheric NO₂ columns decreased across the Iberian Peninsula during the lockdown and full relaxation periods relative to both the pre-pandemic period and the respective periods in 2019 (Figure 8). The relative reductions in TROPOMI/surface levels during the lockdown compared to the same period in 2019 reached 48/51% in BCN and MAD and 49/60, 44/49, 42/41, 43/53, 17/51, 24/40, 19/30, 30/47, and 27/-41% in VAL, MAL, MUR, SEV, MAL, ZAR, COR, BIL, and VLD, respectively. There following represent large differences in the ratios of TROPOMI to surface NO₂ reductions across cities: 0.3–0.6 in BAD, ZAR, BIL, and COR, 0.7–0.8 in VLD, SEV, VAL, and MAL, and 0.9–1.0 in BCN, MAD, and MUR. Barré et al. (2020) also observed this mismatch with TROPOMI/surface level reductions of 8/47, 34/63, and 16/63% for ZAR, VAL, and MAL, respectively; however, their specific causes were not discussed. This discrepancy between the two measurements was also observed when comparing inter-annual trends in the Guadalquivir Valley, which was attributed to intensive agricultural biomass burning emissions affecting TROPOMI NO₂ columns more greatly than urban NO₂ levels (Massagué et al., 2021). In areas where NO_x-traffic sources are dominant, both measurements yielded similar NO₂ changes; however, larger discrepancies were found where the biomass burning sources are relevant (BAD, COR, ZAR, and VLD).

Primary NO_x emissions from traffic (mostly from diesel engines) are dominated by NO rather than NO₂ (approx. 90–75% versus 10–25%, Carslaw et al., 2016). This explains the even stronger reductions in NO during the lockdown when compared to the 2015–2019 averages. In VAL, BCN, MAD, MAL, SEV, and BAD, reductions ranged from 61–72%, while reductions in the other cities varied from 39–49%, except for MUR (26%, Figure 5c). Again, the decreases persisted during the full relaxation period, reaching 43–53% in MAD, COR, BAD, and SEV, 31–35% in BCN, MAL, VAL, VLD, and ZAR, 17% in BIL, and 0% in MUR. Decreases in NO₂ were

greater in the TR and UB sites, with reductions of up to 73 and 75% at TR sites in SEV and MAD, respectively (Table 2).

3.2.2. CO

According to the EU-28 emission inventory, approximately 50, 19, 16, and 12% of the CO emissions arise from domestic, road traffic (mostly petrol-fueled vehicles), energy production and use, and industrial sources (EEA, 2019), respectively. However, agricultural burns may also be a relevant source (Clerbaux et al., 2008).

Metropolitan levels of CO during the pre-pandemic period reached mean values of 267–563 $\mu\text{g}/\text{m}^3$ among urban sites in MAD, BCN, SEV, BCN, BIL, MAL, and VLD and 165–235 $\mu\text{g}/\text{m}^3$ among sites in BAD, COR, MAL, and ZAR (Figure 9a). During the lockdown and full relaxation periods, these levels dropped to 100–428 $\mu\text{g}/\text{m}^3$ for all cities, with higher concentrations recorded in MAD, SEV, MAL, and VLD (some of the largest and mid-sized cities).

Average concentrations of this pollutant compared to the 2015–2019 averages varied widely across Spain. During the lockdown, decreases of 5–23% occurred in MAL, VAL, ZAR, MAD, BIL, BCN, and MUR, while moderate increases (2 and 10% in BAD and SEV, respectively) and large increases (27 and 40% in VLD and COR, respectively) were observed in other areas (Figure 9a and Table 3). During the full relaxation, reductions in CO concentrations still reached 2–18% in BCN, VAL, BIL, COR, and MUR, while increases of 5–46% were observed in ZAR, MAD, MAL, SEV, BAD, and VLD (Figure 9a and Table 3). The reductions were more pronounced at some TR sites (e.g., BCN reached a 43% reduction during the lockdown), while increases were registered at some RUR, UB, and TR sites (i.e., increases of 100 and 123% at RUR sites in MAD as well as 76 and 116% at TR sites in SEV) during the lockdown and full relaxation periods, respectively (Table 3).

The consistent differences among the cities are attributed to a major road traffic origin in most of the largest cities, resulting in a more or less pronounced CO decrease. The increases recorded in several cities during the lockdown and/or full relaxation periods (BAD, VLD, MAL, ZAR, SEV, and MAD) are likely related to an increase in domestic and agricultural biomass burning during the “stay at home” period. In the case of MUR, the large impact of agricultural biomass burns upon air quality is well known (BORM, 2020). In the final stage of the lockdown (06/05/2020), burns were forbidden until 30/09/2020 due to their impact on air quality, which resulted in a greater CO decrease during the full relaxation period (32%) than during the lockdown (23%). Notably, BAD and VLD are located in areas with widespread domestic and agricultural burning. In ZAR, MAD, and MAL, the relative weight of traffic and biomass burning is more balanced.

3.2.3. SO₂

Sulfur dioxide is emitted by high-temperature processes. For instance, 69, 17, and 11% of the SO₂ in the EU-28 emission inventory are attributed to energy production and use, domestic sources, and industry, respectively (EEA, 2019). The highest concentrations are reached where coal stoves are still used (e.g., the old city center of MAD). In BCN, SO₂ levels are markedly lower and peak when harbor shipping emissions affect urban air quality under sea breeze circulation.

SO₂ is a pollutant present in relatively low concentrations, with averages during the different periods of the lockdown and full relaxation ranging from <1–2 µg/m³ in BAD and BCN, 3–4 µg/m³ in ZAR, SEV, and VAL, and 5–7 µg/m³ in BIL, COR, MAD, MAL, MUR, and VLD (Table 3). The results obtained for the first four cities should be taken with caution due to the relatively high detection limits of conventional SO₂ analyzers. Considering these important limitations, a generalized decrease was recorded during the lockdown when compared to 2015–2019 averages over the same period (Figure 9b and Table 4). Reductions reached 25–35% in the metropolitan areas of BCN, MAL, SEV, MAD, and BIL and 4 to –16% in VAL, VLD, MUR, and COR. Only ZAR recorded slight increases in SO₂ (6%). During the full relaxation, levels also decreased in most cities (e.g., decreases from 7–18% in COR, MAD, MUR, and MAL to 25 and –26% in BCN and SEV, respectively). Incremental increases were also registered in some cases (i.e., increases of 5 to –18% in VAL, ZAR, BIL, and VLD; Figure 9b and Table 3).

Most relative decreases in SO₂ during restriction periods can be attributed to a decline in specific industrial emissions, and—in some cases—to shipping (mainly cruises since cargo shipping was less affected). While such increases could be also attributed to industrial (VLD and ZAR) and/or shipping emissions (COR and BIL both have a nearby petrochemical plant and harbor), the increased domestic contributions from scarce coal stoves cannot be discarded in some cities from central Spain (e.g., ZAR). Furthermore, in cities with harbors, the constant number of ships (e.g., VAL) or the increased number of fishing vessels (e.g., COR, especially during the full relaxation period) resulted in a smaller decrease—or even an increase—in SO₂ concentrations.

3.2.4. NH₃

While ammonia is a gaseous atmospheric pollutant emitted from different sources, agriculture and farming globally represent the major sources of NH₃ (Behera et al., 2013). In the emission inventory of EU-28, 92% of NH₃ emissions were attributed to agriculture and farming, with the domestic, industry, road traffic, and waste management sectors contributing 1–2% each (EEA, 2019). Ammonia is an alkaline gas with a very large effect on the generation of fine PM via its interaction with acidic species such as HNO₃ and H₂SO₄ (Backes et al., 2016). Traffic emissions arise from gasoline vehicles and the NH₃ slip of selective catalytic reduction controls in diesel vehicles (Suarez-Bermejo et al., 2014). These might have special relevance for urban PM because they are emitted with acidic species. Data for urban NH₃ were only available for TR sites in VAL (5–6 µg/m³) and BIL (2–4 µg/m³). During the lockdown, these levels were reduced by 9% in VAL and by 38% in BIL. During the full relaxation, the reductions were 3 and 33% in VAL and BIL, respectively (Table 3). Furthermore, Reche et al. (2015) noted higher summer NH₃ concentrations in Spanish cities associated with organic city waste management. This could explain the higher levels in VAL (warmer) than in BIL; however, the higher regional farming/agricultural emissions in VAL could also contribute to this result (Van Damme et al., 2018).

3.2.5. O₃

Ozone is a complex secondary pollutant generated in the atmosphere from volatile organic compounds (VOCs) and NO_x via photochemically driven reactions (Monks et al., 2015, and references therein). During the pre-pandemic stage, averaged 8hDM O₃ levels (Figure 10a) were typically higher in the NW, W, SW, and S regions of Spain (65 to 87 µg/m³) than in the E

regions (58 to 67 $\mu\text{g}/\text{m}^3$). During the lockdown, 8hDM O_3 levels increased in both regions, reaching 74–89 $\mu\text{g}/\text{m}^3$ in the W and SW and 72–90 $\mu\text{g}/\text{m}^3$ in the NE. Despite a larger increase in the NE, the values remained lower than in the W, SW, and S. Notably, while O_3 levels in Spain normally peak in June–July (Querol et al., 2016), mobility remained below typical levels during the full relaxation period (17 and 27% lower in BCN and MAD, respectively, for the average weekday vehicles; 25 and 38% lower for MAL and MAD, respectively, based on Google mobility index data). Thus, between the lockdown and full relaxation—which coincided with the O_3 maxima season—average metropolitan levels of 8hDM O_3 grew from 73 to 76 $\mu\text{g}/\text{m}^3$ in the N and W borders (COR and BIL), from 83 to 87 $\mu\text{g}/\text{m}^3$ in the NE, E, and SE areas (ZAR, BCN, VAL, and MUR), and from 98 to 101 $\mu\text{g}/\text{m}^3$ in the C (central) and S regions (BAD, MAD, SEV, and MAL) (Figure 10a). This geographical distribution of O_3 is typical in mainland Spain due to climatological factors. Although the beginning of the full relaxation in June 2020 was wetter and more unstable than usual, the meteorological condition in July returned to near-climatological values for most of the territory.

Regarding the receptors of metropolitan pollution, we observed similar levels of 8hDM O_3 to those recorded in cities during the pre-pandemic stage, reaching 65 (COR) to 79 (SEV) $\mu\text{g}/\text{m}^3$ in the W half of Spain and 80 (BIL) to 89 (MAL) $\mu\text{g}/\text{m}^3$ in the E half of Spain, except in BCN and MUR (63 and 69 $\mu\text{g}/\text{m}^3$, respectively) (Figure 10c). The high O_3 levels in MAL during this period coincided with a positive temperature anomaly over this area (see Figure 4). During the lockdown, these receptor areas recorded levels from 72–83 $\mu\text{g}/\text{m}^3$, except for the most N, C, and S ones (BIL, SEV, MAD, and MAL; 87–90 $\mu\text{g}/\text{m}^3$) (Figure 10c). During the full relaxation, averaged 8hDM O_3 levels at the receptor areas increased up to 90–96 $\mu\text{g}/\text{m}^3$ in the N half of the peninsula (BCN, VAL, BIL, ZAR, and VLD), and up to 102–107 $\mu\text{g}/\text{m}^3$ in the C and S regions (MAD, MAL, SEV, and BAD; Figure 10c).

Reductions in the averaged metropolitan 8hDM O_3 levels during the lockdown relative to the 2015–2019 period (Figure 10a and Table 4) ranged from -7 to -17% in most cities (VAL, SEV, MAD, COR, ZAR, BAD, MUR, and VLD). In MAL, BCN, and BIL, the changes were small and ranged from -3 to +2%. While the meteorology-normalized reductions exhibited the same spatial patterns, the magnitude of the reductions was smaller and the increases were more pronounced. In summary, by canceling out the effect of meteorology (Figure 10b and Table 4), five metropolises (VAL, ZAR, COR, BAD, and VLD) showed O_3 decreases ranging from -4 to -13%, while six other cities (MAL, MAD, SEV, MUR, BIL, and BCN) either did not experience relevant reductions or suffered increases (-2 to +10%).

During the full relaxation, 8hDM O_3 levels were between 4 and 18% lower in comparison to 2015–2019 averages for cities located in C and E Iberia (VAL, MAL, MAD, ZAR, BCN, VLD, and MUR), and either increased or barely changed in the N coast and the W regions (+8% in BIL and -1 to -3% in SEV, COR, and BAD) (Figure 10a and Table 4). The meteorology-normalized data again showed a generalized reduction during this late period for five metropolises (reductions of 4–10% MAD, VAL, MUR, VLD, and ZAR), minor changes in others (-3% for COR and MAL; -2% for BCN and BAD; +1% for SEV) and a marked increase (14%) in BIL (Figure 10b and Table 4).

During the full relaxation, most receptor areas presented levels that were 5 (BAD) to 19% (BCN) lower, with larger reductions in the E half of Spain. Only VLD and SEV did not change greatly (+3 to -1%) (Figure 10c and Table 4). The 40% reduction in MUR seems to be due to local

reasons (e.g., O₃ titration) since it was only observed in one station of the set selected for this metropolis. The meteorology-normalized data show the same pattern, with 4–14% reductions for the cities of E side (including MAD and BIL, and excluding 30% for MUR) and no major changes in the W side (1% reduction for COR and SEV, 0% for BAD, and a 2% increase in VLD) (Figure 10d and Table 4). We observed average reductions in 8hDM O₃ levels for the E side of Spain (approximately 12%) in the maximum O₃ season coinciding with a 15–25% traffic reduction in cities. In urban areas, the decrease was close to 6% on average; however, an increase of 14% was recorded in BIL.

Our O₃ results are subject to higher uncertainty than those of other pollutants due to the photochemical dependence of O₃, the specific meteorological scenarios favoring O₃ episodes in the Mediterranean (Millán et al., 1997, 2002; Gangoiti et al., 2001; Millán, 2014; Querol et al., 2017, 2018; Massagué et al., 2019, among others), and the marked inter-annual variability. However, the results suggest a generalized decrease in 8hDM O₃, which was more pronounced in E Spain. However, the WHOAQG of 100 µg/m³ for the 8hDM was still exceeded, even when mobility was reduced by approximately 65 and 20–35% during the lockdown and full relaxation periods, respectively. This typically occurred in receptor areas in C and S Spain (BAD, MAL, MAD, and SEV) and in some urban areas (SEV, MAD, and MAL). The meteorological analysis results suggest that the C, W, and S regions of Spain recorded positive anomalies for temperature and negative anomalies for wind speeds in June and July, thus favoring O₃ formation and accumulation. In the rest of Spain, a -3°C average temperature anomaly was registered with positive anomalies of cloud cover and precipitation, which might have resulted in lower O₃ levels. As a result, higher than usual concentrations in central and S Spain, as well as marked decreases in the E side, can be attributed to a combined effect of lower precursor emissions and the observed temperature, cloud cover, and precipitation anomalies affecting the E regions in June 2020 when atypical, unstable and wet weather occurred (see the meteorology-corrected data below).

The metropolitan area reductions in 8hDM levels did not follow a clear geographical pattern—even within several cities increases or lack of variation were observed. These differences can be attributed to differing VOCs- or NO_x-limiting environments or differences in the relative balance between NO titration and VOCs ozonolysis decrease/O₃ formation decreases. Increases in O₃ within urban areas during lockdowns have already been reported elsewhere (e.g., China, +36%; Europe, +17%; Sicard et al., 2020), even after canceling out the effect of meteorology (Zhao et al., 2020); however, our results are not directly comparable with the results of Sicard et al. (2020). Notably, Sicard et al. (2020) observed an increase in daily means, which includes night periods that are highly affected by titration and ozonolysis (and thus cannot be directly compared to our data (using 8hDM)). Also, in contrast to those studies, our results include data from the month of July, when most Iberia experience the maximum frequency and intensity of O₃ episodes (Querol et al., 2016).

Under relatively low photochemical activity (such as during the lockdown), O₃ can increase due to reduced O₃ consumption by titration and ozonolysis prevailing over a higher local O₃ production due to the decrease of NO_x in a VOCs-limited environment since long-range transport O₃ typically prevails over local production. In summer, when most acute O₃ episodes occur, both the reduction of NO emissions associated with the pandemic restrictions and VOC-limited O₃ formation might have also generated a net positive anomaly in several metropolitan

areas. In any case, increases and weak decreases are more frequent at UB and TR sites. Notably, meteorology-normalized variations of +2 and -1% as well as -1 and -4% were estimated during the lockdown and full relaxation, respectively, as averages for the 11 metropolises (Table 3). However, at the receptor sites, decreases were more pronounced (average: 7% across the 11 regions) during both the lockdown and full relaxation periods (Table 3). Positive anomalies occurring in urban areas with larger populations are problematic because health effects are far more important since they affect more people. Thus, for the net effects of the O₃ changes concerning health outcomes, affected populations should also be considered.

3.2.6. PM₁₀ and PM_{2.5}

According to the receptor modeling source, apportionment studies performed in S European urban areas, including BCN, suggest that 30–35% of the UB annual PM₁₀ and PM_{2.5} averages are attributable to road traffic, with the secondary PM fraction representing 50–60% of PM₁₀ and 65–70% of PM_{2.5} (Amato et al., 2016). Thus, both—but especially PM_{2.5}—are driven by secondary components and have a high degree of complexity. Furthermore, Spain is frequently affected by N African dust outbreaks that could greatly influence PM levels (Querol et al., 2019a and b). Calculations were performed for four parameters: PM₁₀, PM_{2.5}, and both fractions following the subtraction of African dust contributions (PM_{10sub} and PM_{2.5sub}); however, only the ones with the subtraction are discussed here.

Averaged metropolitan PM_{10sub} levels during the pre-pandemic period ranged from 12–16 µg/m³ in ZAR, BAD, SEV, and MAD, 20–25 µg/m³ in MUR, VLD, BIL, VAL, and BCN, and reached 31 µg/m³ in COR. During the lockdown, levels were reduced to 7–11 µg/m³, except in BCN, BIL, and COR, where they reached 15, 15, and 20 µg/m³, respectively (Figure 11a). While PM_{10sub} increased during the full relaxation period, the same ranking of metropolitan areas was obtained, ranging from 15–21 µg/m³ in most cities, except for ZAR, MAD, and COR, which had PM_{10sub} values of 9, 13, and 24 µg/m³, respectively (Figure 11a).

For PM_{2.5sub}, the variability across most metropolitan areas during the pre-pandemic was lower (11–13 µg/m³), except for BCN (19 µg/m³) and VAL (17 µg/m³). During the lockdown, MAD, COR, VLD, and V. L. reached values of 7–10 µg/m³, while BIL, ZAR, and BCN reached 11–13 µg/m³, and most metropolises reached 8–9 µg/m³—except BCN (12 µg/m³)—during the full relaxation period. The PM_{2.5sub} (Figure 11b) levels did not change (0 to -1 µg/m³) compared to the bulk PM_{2.5} levels since African dust has a dominant coarser size mode.

When compared to 2015–2019, PM_{10sub} levels in most metropolitan areas experienced a 31% (MAD) to 47% (ZAR) decrease during the lockdown, except for COR (-12%), VLD and BIL (-8 and -9%, respectively), and MUR (0%) (Figure 11a and Table 4). This general reduction was softened during the full relaxation period, with four out of the nine cities experiencing PM_{10sub} decreases of 19–38% (BCN, SEV, MAD, and ZAR), while COR and BIL by experienced decreases of 8 and 10%, respectively. Notably, PM_{10sub} increases of 3, 5, and 47% were observed in VAL, MUR, and VLD, respectively (Figure 11a and Table 4). Information is scarce for PM_{2.5sub} because PM_{2.5} is measured using gravimetric methods in several areas and data availability is delayed in some cases. The available data shows a weaker reduction during the lockdown when compared to 2015–2019, with +3% in BIL, -3% in ZAR, -10 to -25% in MAD, VLD,

BCN, VAL, and COR, +7% in VLD, and -8 to -13% for the other cities during the full relaxation period (Figure 11b and Table 4).

After meteorological normalization, PM_{2.5sub} reduction patterns during the lockdown changed significantly, with changes of +3% in BIL, 0% in ZAR, -1% in VLD, -10% in MAD, and -28 to -39% in BCN, COR, and VAL. During the full relaxation period, PM_{2.5sub} changed by +25 to +2% in ZAR, VLD, and BIL, by -4% in MAD, and by -15 to -38% in VAL, BCN, and COR (Figure 11c and Table 4). In summary, the results show consistent reductions in PM_{10sub} and PM_{2.5sub} in BCN, MAD, VAL, SEV, and COR, particularly during the lockdown. The difference between the anomalies with and without meteorological normalization is due to the high impact of specific meteorological conditions such as rainfall, humidity temperature, and insolation on the formation of PM_{2.5}, which is dominated by secondary organic and inorganic aerosols.

The results show that, on average, in six out of the ten metropolitan areas, the PM₁₀ annual WHOAQG of 20 µg/m³ was reached or exceeded by PM_{10sub} during the pre-pandemic period. While exceedances of averaged PM_{10sub} did not occur during the lockdown, levels were higher in BIL, BCN, MUR (15 µg/m³), and COR (20 µg/m³). In COR, high levels are likely related to sea spray contributions, which are known to greatly contribute to the annual mean PM₁₀ in the metropolis (Fernández-Amado et al., 2018), and the low PM_{2.5}/PM₁₀ (0.4) obtained in this study.

For PM_{2.5sub}, the annual PM_{2.5} WHOAQG of 10 µg/m³ was surpassed in most cities during the pre-pandemic period. During the lockdown, BCN reached 12 µg/m³, while COR, BIL, and ZAR reached similar levels (9 µg/m³). During the full relaxation, BCN reached 13 µg/m³, while COR, VAL, VLD, and ZAR were also close to the limit value (9–10 µg/m³) (Figure 11). This highlights the potential relevance of non-vehicular regional emissions on secondary PM precursors or other emission sources such as industry, agriculture/farming, and domestic or agricultural biomass emissions. Areas exceeding the annual PM_{2.5} WHOAQG are characterized by relatively high industrial densities with emissions of primary PM and gaseous precursors. Moreover, BCN and ZAR are located in an NH₃ hotspot region due to farming and agricultural emissions (Van Damme et al., 2018) that might have favored the formation of secondary PM during the lockdown, especially ammonium nitrate (NH₄NO₃), compared with other areas. The thermal stability of NH₄NO₃ is low at ambient temperatures exceeding 25°C (Pio & Harrison, 1984), which can explain why the geographic differences in PM_{2.5sub} levels were reduced in the much warmer full relaxation period when compared to the pre-pandemic and lockdown periods.

In metropolitan areas, PM₁₀ is more strongly affected by local emissions (e.g., traffic including resuspension, building works, industry, etc.) than PM_{2.5}, which is mostly secondary and of regional origin (Amato et al., 2016, among others). Thus, in the large cities under consideration, namely MAD, BCN, SEV, and ZAR, PM_{10sub} anomalies during the lockdown reached -31 to -47%, while PM_{2.5sub} only changed by -3 to -22%.

Considering that the average road traffic contribution to PM₁₀ and PM_{2.5} in most European cities is 27 and 30% for UB and TR sites (Amato et al., 2016), respectively, we can roughly estimate that with 65 and 20% traffic reductions during the lockdown and full relaxation periods, respectively, the expected reductions should have been around 17 and 5% for PM_{10sub}, and 19 and 6% for PM_{2.5sub} during the two periods, respectively. The average meteorology-normalized reduction of PM_{2.5sub} reached 17 and 6% during the lockdown and

full relaxation periods, respectively (close to the expected reductions); however, large differences were observed across metropolises. In BCN, COR, and VAL, $PM_{2.5sub}$ fell by 28–43% and by 25–32% during the lockdown and full relaxation periods, respectively. In these cities, the additional reduction of emissions (industrial, harbors) must be considered to explain the higher than expected reductions. On the other hand, in MAD, BIL, VLD, and ZAR, the levels were reduced less than expected or even increased. The latter is likely related to increases in emissions (e.g., domestic and agricultural biomass burning, among others) consistent with the increases in CO and SO₂ concentrations. Additionally, as reported during lockdowns in other metropolitan areas (Huang et al., 2020; Le et al., 2020; Chen et al., 2020; Silver et al., 2020; Nakada et al., 2020), specific atmospheric conditions favoring the formation of secondary PM at regional levels during the lockdown may explain these moderate decreases or increases. Huang et al. (2020) and Le et al. (2020) described anomalously high $PM_{2.5}$ episodes in China during the COVID-19 lockdown period and used modeling to determine that these were due to meteorological conditions favoring the formation of secondary PM from gaseous precursors. Decreases in NO_x emissions from transportation in urban VOCs-limited O₃ formation environments might have favored a rise in O₃ concentrations in a number of cities. Urban O₃ increases have been reported as increasing OH radicals during the day and NO₃ radicals in the night (Saiz-López et al., 2017), thereby increasing the atmospheric oxidizing capacity and resulting in increased secondary PM. This secondary PM relative load increases with growing distance from urban areas and can represent a high proportion at the receptor sites, where the $PM_{2.5}$ anomalies were negative in some cases but positive in others (-10 and -26% in COR and VAL, but 3 and 6% in BIL and MAD for $PM_{2.5sub}$, respectively in the lockdown; Figure 11, Table 4). In most cases, marked decreases were recorded at TR sites where the proportion of secondary PM was minimal. On average, these reductions ranged between 15 and 26% for PM_{10sub} and $PM_{2.5sub}$ in the considered cities during the lockdown, and 20% $PM_{2.5sub}$ reductions were after canceling out the effect of meteorology (Table 4). Furthermore, the aforementioned increase in urban freight distribution vehicles (mostly diesel and relatively old, without filter traps) might have also moderated the decreases in $PM_{2.5sub}$ and PM_{10sub} at traffic sites.

4. CONCLUSIONS

The reduction of emissions associated with mobility restrictions and other human activities implemented during the COVID-19 pandemic has provided a unique opportunity to evaluate the impact of such drastic events on air quality and learn lessons for the design of effective air quality policies. Using experimental data, we have evaluated this impact for several Spanish metropolitan and surrounding rural areas. We anticipate that understanding the effect of such emission reductions on secondary pollutants such as O₃ and $PM_{2.5}$ will require the application of chemical and dispersion modeling tools. In this context, COVID-19 emission reductions also provide a unique opportunity to constrain the models used to anticipate the potential benefits or policy-based emission reductions. In this section, we synthesize the major trends observed and make suggestions for future policies on air quality management in Spain.

In BCN, we found that a relevant fraction of commuters changed their transport mode from public transport to private cars during the full relaxation period, which was likely due to the fear of SARS-CoV-2 infection. Notably, this shift in transport mode should be reverted as soon as possible.

As described in many other regions of the world, levels of most pollutants decreased in Spain due to COVID-19 restrictions, with traffic falling by up to 80% during the full lockdown. Thus, for combustion-related primary or mainly primary pollutants such as NO_2 , CO , and SO_2 , a widespread decreasing trend was evidenced, especially for those pollutants most commonly associated with road traffic. For example, NO_2 levels during the lockdown reached values below half of the annual WHO's air quality guideline (WHO AQG). Results for BCN also indicated that traffic flow should be reduced by 30% (with the current fleet composition) to avoid exceeding this annual guideline. In the cases of CO and SO_2 , the "COVID-19 effect" was sometimes less obvious, which was likely due to two major factors. First, because levels of CO and SO_2 are relatively low in many stations, the detection limit and maintenance protocols may have affected measurements, thereby making it difficult to observe clear trends. In the light of this observation, we strongly recommend adapting the instrumentation to meet more stringent requirements for measuring relatively low concentrations of these pollutants. Second, in some cases, the effect of industrial/shipping/power generation, agricultural and domestic biomass burning (CO), and sporadic domestic coal burning (SO_2) were likely responsible for a lower than expected COVID-19-related reduction.

For O_3 , we considered more relevant to evaluate emission reductions during the full relaxation period (June-July) coinciding with the maximum O_3 period in Spain (when mobility reduction remained close to 20%) than during the full lockdown (March). In June-July, the meteorology-normalized data showed a generalized reduction in 8hDM O_3 of 4–10% in MAD, VAL, MUR, VLD, and ZAR, only minor reductions in COR and BIL (3%) as well as BCN and BAD (2%), while increases were observed in SEV (1%) and BIL (14%). In the receptor areas, levels were reduced by 4–14% in the most cities of C and E Spain (including MAD and BIL and excluding 30% in MUR), with no major changes in the more W areas (-1% in COR and SEV, 0% in BAD and +2% in VLD). In the E side of Spain, we observed average reductions in 8hDM O_3 levels of approximately 12% during the maximum O_3 season, which coincided with a 15–25% reduction in city traffic. While the average reduction approached 6% in urban areas, an increase of 14% was recorded in BIL. Thus, mobility reductions of approximately 20% during this high O_3 period reduced O_3 levels, especially in the rural or suburban receptor sites. However, it is also relevant that the WHO AQG of $100 \mu\text{g}/\text{m}^3$ for the 8hDM was still exceeded, even when mobility was reduced by approximately 65 and 20–35% during the lockdown and full relaxation periods, respectively. For secondary pollutants such as O_3 , further research should include chemical and dispersion modeling, along with source apportionment techniques, to suggest major precursor reduction targets. This should be performed for various atmospheric basins and cities that have different emission and climatic patterns.

For $\text{PM}_{2.5}$, which is mostly secondary in origin, the results demonstrated a much less pronounced reduction than for NO_2 due to the lower contribution of traffic-related $\text{PM}_{2.5}$ and the relatively higher contribution of non-vehicular regional emissions on secondary PM precursors or other pollutant sources such as industry, agriculture/farming, and domestic biomass emissions. Some cities exceeded the annual $\text{PM}_{2.5}$ WHO AQG during the lockdown due to their relatively high industrial activity producing emissions of primary PM and gaseous precursors. Moreover, some of these cities (i.e., BCN and ZAR) are located in an NH_3 hotspot region due to farming and agricultural emissions, which might have favored the formation of secondary PM during the lockdown. In such areas, more vigorous air quality policies aimed at

abating gaseous precursors from combustion (including domestic and agricultural biomass burning) and farming/agriculture would ensure success in achieving the PM_{2.5} WHOAQG.

For PM₁₀, the annual WHOAQG was not exceeded during the lockdown, and there was a more marked decrease in PM₁₀ when compared to PM_{2.5} (but still less pronounced than for NO₂), which we attribute to reduced emissions from road dust, vehicle wear, and construction/demolition activities. Thus, these sources must be strongly considered in urban air quality policies. It is also relevant to mention the high impact of sea salt on average lockdown PM₁₀ levels on the NW coast of Spain.

ACKNOWLEDGMENTS

The present work was supported by the Spanish Ministerio para la Transición Ecológica y Reto Demográfico (17CAES010), the “Agencia Estatal de Investigación” from the Spanish Ministry of Science and Innovation (IDAEA-CSIC is a Centre of Excellence Severo Ochoa CEX2018-000794-S), FEDER funds under the project CAIAC (PID2019-108990RB-100), and by the Generalitat de Catalunya (AGAUR 2017 SGR41). We would like to thank the Spanish Meteorological Office (AEMET) for providing meteorological data as well as NASA for providing OMI-NO₂ data. BSC co-authors acknowledge the support of the Copernicus Atmosphere Monitoring Service (CAMS), which is implemented by the European Centre for Medium-Range Weather Forecasts (ECMWF) on behalf of the European Commission, the Ministerio de Ciencia, Innovación y Universidades (MICINN) (RTI2018-099894-B-I00, CGL2017-88911-R), the Agencia Estatal de Investigación (PID2019-108086RA-I00/AEI/10.13039/501100011033), the AXA Research Fund, and PRACE and RES for awarding access to Marenostrum4 based in Spain at the Barcelona Supercomputing Center. H. Petetin also acknowledges the European Union’s Horizon 2020 research and innovation program under the Marie Skłodowska-Curie grant agreement H2020-MSCACOFUND-2016-754433.

REFERENCES

- AENA, 2020. Aeropuertos Españoles y Navegación Aérea. Estadística del tráfico aéreo: Informe 2019. http://www.aena.es/csee/ccurl/174/519/00.Definitivo_2019.pdf
- Amato, F., Alastuey, A., Karanasiou, A., Lucarelli, F., Nava, S., Calzolari, G., Severi, M., Becagli, S., Gianelle, V. L., Colombi, C., Alves, C., Custódio, D., Nunes, T., Cerqueira, M., Pio, C., Eleftheriadis, K., Diapouli, E., Reche, C., Minguillón, M. C., Manousakas, M.-I., Maggos, T., Vratolis, S., Harrison, R. M., and Querol, X., 2016. AIRUSE-LIFE+: a harmonized PM speciation and source apportionment in five southern European cities, *Atmos. Chem. Phys.*, 16, 3289–3309, <https://doi.org/10.5194/acp-16-3289-2016>
- Backes A.M., Aulinger A., Bieser J., Matthias V., Quante M., 2016. Ammonia emissions in Europe, part II: How ammonia emission abatement strategies affect secondary aerosols. *Atmospheric Environment*, 126, 153-161.
- Baldasano, J. COVID-19 lockdown effects on air quality by NO₂ in the cities of Barcelona and Madrid (Spain). *Science of the total environment*, 2020, 741, 140353.
- Barré, J., Petetin, H., Colette, A., Guevara, M., Peuch, V.-H., Rouil, L., Engelen, R., Inness, A., Flemming, J., Pérez García-Pando, C., Bowdalo, D., Meleux, F., Geels, C., Christensen, J. H., Gauss, M., Benedictow, A., Tsyro, S., Friese, E., Struzewska, J., Kaminski, J. W., Douros, J.,

- Timmermans, R., Robertson, L., Adani, M., Jorba, O., Joly, M., and Kouznetsov, R., 2020. Estimating lockdown induced European NO₂ changes, *Atmos. Chem. Phys. Discuss.*, <https://doi.org/10.5194/acp-2020-995>
- Bauwens, M. S. Compernelle, T. Stavrakou, J.-F. Müller, J. van Gent, H. Eskes, P. F. Levelt, R. van der A, J. P. Veefkind, J. Vlietinck, H. Yu, C. Zehner: Impact of coronavirus outbreak on NO₂ pollution assessed using TROPOMI and OMI observations. *Geophysical Research Letters*, <https://doi.org/10.1029/2020GL087978>, 2020.
- BCC, 2016. Barcelona City Council. Programa de mesures contra la contaminació de l'aire, 33 pp. <https://media-edg.barcelona.cat/wp-content/uploads/2016/11/AireNetBCN.pdf>
- Behera S.N., Sharma M., Aneja V.P., Balasubramanian R., 2013. Ammonia in the atmosphere: a review on emission sources, atmospheric chemistry and deposition on terrestrial bodies. *Environ Sci Pollut Res* 20, 8092–8131.
- BORM, 2020. Official Bulletin of the Murcia Region. 06/05/2020. <https://www.borm.es/servicios/anuncio/ano/2020/numero/202011/pdf?id=784621>
- Carlsaw D.C., Murrells T.P., Andersson J., Keenan M., 2016. Have vehicle emissions of primary NO₂ peaked? *Faraday Discussions*, 189, 439-454.
- Chakraborty, I. & Maity, P. (2020). COVID-19 outbreak: migration, effects on society, global environment and prevention. *Science of the Total Environment*, 728, 13882.
- Chen H., Huo J. Fu Q., Duan Y., Xiao H., Chena J., Impact of quarantine measures on chemical compositions of PM_{2.5} during the COVID-19 epidemic in Shanghai, China. *Science of The Total Environment*, 748, 15, 2020, 140758. <https://doi.org/10.1016/j.scitotenv.2020.140758>
- Clerbaux C., Edwards D.P., Deeter M., Emmons L., Lamarque J.F., Tie X.X., Massie S.T., Gille J., 2008. Carbon monoxide pollution from cities and urban areas observed by the Terra/MOPITT mission. *Geophysical Research Letters*, 35, L03817, doi:10.1029/2007GL032300.
- Collivignarelli, M. C., A. Abba, G. Bertanza, R. Pedrazzani, P. Ricciardi, and M. C. Miino: Lockdown for CoViD-2019 in Milan: What are the effects on air quality? *Science of the Total Environment*, 732 (139280), <https://doi.org/10.1016/j.scitotenv.2020.139280>, 2020.
- DGT, 2020. Dirección General de Tráfico: Parque de vehículos - Anuario – 2019. <http://www.dgt.es/web/seguridad-vial/estadisticas-e-indicadores/parque-vehiculos/tablas-estadisticas/2019/> (accessed 29/10/2020)
- Doty, B. E., & Kinter, J. L. III (1995). In E. P. Szuszczewicz, & J. H. Bredekamp (Eds.), *Geophysical data analysis and visualization using GrADS. Visualization techniques in space and atmospheric sciences* (pp. 209–219). Washington, DC: NASA.
- EC, 2018. Directive 2008/50/EC of the European Parliament and of the Council of 21 May 2008 on ambient air quality and cleaner air for Europe, OJ L 152, 11.6.2008,44 pp,
- EEA, 2019. EEA (2019). Air quality in Europe — 2019. European Environmental Agency, Report 10/2019. 99 pp, <https://www.eea.europa.eu/publications/air-quality-in-europe-2019>.
- Escudero, M., Querol, X., Pey, J., Alastuey, A., Pérez, N., Ferreira, F., Alonso, S., Rodríguez, S. and Cuevas, E.: A methodology for the quantification of the net African dust load in air quality monitoring networks, *Atmos. Environ.* 41, 5516-5524, 2007.
- Escudero, M., Segers, A., Kranenburg, R., Querol, X., Alastuey, A., Borge, R., de la Paz, D., Gangoiti, G., and Schaap, M.: Analysis of summer O₃ in the Madrid air basin with the

- LOTOS-EUROS chemical transport model, *Atmos. Chem. Phys.*, 19, 14211–14232, doi: 10.5194/acp-19-14211-2019, 2019.
- Fernández-Amado, M.; Prieto-Blanco, M. C.; López-Mahía, P.; Piñeiro-Iglesias, M.; Muniategui-Lorenzo, S.; Iglesias-Samitier, S.; Alves, C. A.; Custódio, D.; Esteves, V.; Nunes, T., 2018. Interrelationships between major components of PM₁₀ and sub-micron particles: Influence of Atlantic air masses. *Atmospheric Research*, 212, 64-76 DOI: 10.1016/j.atmosres.2018.05.003
- Gangoiti, G., Alonso, L., Navazo, M., Albizuri, A., Perez-Landa, G., Matabuena, M., Valdenebro, V., Maruri, M., Antonio García, J. and Millán, M. M., 2001. Regional transport of pollutants over the Bay of Biscay: Analysis of an ozone episode under a blocking anticyclone in west-central Europe. *Atmospheric Environment*, 36, 8, 1349–1361.
- Gkikas A., Houssos E.E., Lolis C.J., Bartzokas A., Mihalopoulos N., Hatzianastassiou N., 2015. Atmospheric circulation evolution related to desert dust episodes over the Mediterranean. *Quarterly Journal of the Royal Meteorological Society* 141, 690, Part A, 1634-1645.
- Google LLC. (2020). Google COVID-19 Community Mobility Reports. Available online at: <https://www.google.com/covid19/mobility>.
- Gorelick, N., Hancher, M., Dixon, M., Ilyushchenko, S., Thau, D., & Moore, R. (2017). Google Earth Engine: Planetary-scale geospatial analysis for everyone. *Remote Sensing of Environment*.
- Guevara, M., Jorba, O., Soret, A., Petetin, H., Bowdalo, D., Serradell, K., Tena, C., Denier van der Gon, H., Kuenen, J., Peuch, V.-H., and Pérez García-Pando, C. (2021) Time-resolved emission reductions for atmospheric chemistry modelling in Europe during the COVID-19 lockdowns, *Atmos. Chem. Phys.*, 21, 773–797, <https://doi.org/10.5194/acp-21-773-2021>.
- Huang X., Ding A., Gao J., Zheng B., Zhu D., Qi X., Tang R., Wang J., Ren Ch., Nie W., Chi., Xu Z., Chen L., Li Y., Che F., Pang N., Wang H., Tong D., Qin W., Cheng W., Liu W., Fu Q., Liu B., Chai F., Davis S.J., Zhang O., He K., 2020. Enhanced secondary pollution offset reduction of primary emissions during COVID-19 lockdown in China. *National Science Review*, nwa137, <https://doi.org/10.1093/nsr/nwaa137>
- IGN, 2018. Clasificación climática según Köppen. Centro Nacional de Información Geográfica. Instituto Geográfico Nacional. Ministerio de Transportes, Movilidad y Agenda Urbana. <http://atlasnacional.ign.es/wane/Clima>
- INE 2020. Estadística estructural de empresas: sector industrial. Instituto Nacional de Estadística, https://www.ine.es/dyngs/INEbase/operacion.htm?c=Estadistica_C&cid=1254736143952&menu=resultados&secc=1254736143612&idp=1254735576715
- John Hopkins University, 2020. COVID-19 Dashboard by the Center for Systems Science and Engineering (CSSE) at Johns Hopkins University (JHU). <https://coronavirus.jhu.edu/map.html> (Accessed 28/10/2020)
- Le Quéré, C., Jackson, R.B., Jones, M.W. et al., 2020. Temporary reduction in daily global CO₂ emissions during the COVID-19 forced confinement. *Nature Clim. Chang.* 10, 647–653. <https://doi.org/10.1038/s41558-020-0797-x>
- Le T., Wang Y., Liu L., Yang J., Yung Y.L., Li G., Seinfeld J.H., 2020. Unexpected air pollution with marked emission reductions during the COVID-19 outbreak in China. *Science* 369, 702–706.

- Liu Z., Ciais P., Deng Z., et al., 2020. Near-real-time monitoring of global CO₂ emissions reveals the effects of the COVID-19 pandemic. *Nature Commun.*, 11, 5172. <https://doi.org/10.1038/s41467-020-18922-7>
- Massagué, J., Carnerero, C., Escudero, M., Baldasano, J. M., Alastuey, A. and Querol, X., 2019. 2005–2017 ozone trends and potential benefits of local measures as deduced from air quality measurements in the north of the Barcelona Metropolitan Area. *Atmospheric Chemistry and Physics*, 19, 7445–7465, <https://doi.org/10.5194/acp-19-7445-2019>
- Massagué, J., Contreras, J., Campos, A., Alastuey, A., Querol, X., 2010. 2005–2018 trends in ozone peak concentrations and spatial contributions in the Guadalquivir Valley, Southern Spain. *Atmospheric Environment*. Submitted
- Millán, M. M., 2014. Extreme hydrometeorological events and climate change predictions in Europe. *Journal of Hydrology*, 518 PB, 206–224.
- Millán, M. M., José Sanz, M., Salvador, R. and Mantilla, E., 2002. Atmospheric dynamics and ozone cycles related to nitrogen deposition in the western Mediterranean. *Environmental Pollution* 118, 2, 167–186.
- Millán, M. M., Salvador, R., Mantilla, E. and Kallos, G., 1997. 'Photooxidant dynamics in the Mediterranean basin in summer: Results from European research projects', *Journal of Geophysical Research Atmospheres*, 102, 7, 8811–8823.
- MITMA, 2020. Áreas Urbanas en España, 2019. Ministerio de Transportes, Movilidad y Agencia Urbana, DG de Vivienda y Suelo. NIPO: 796-10-112-X
- Monks, P. S., Archibald, A. T., Colette, A., Cooper, O., Coyle, M., Derwent, R., Fowler, D., Granier, C., Law, K. S., Mills, G. F., Stevenson, D. S., Tarasova, O., Thouret, V., Von Schneidmesser, E., Sommariva, R., Wild, O. and Williams, M. L., 2015. Tropospheric ozone and its precursors from the urban to the global scale from air quality to short-lived climate forcer. *Atmospheric Chemistry and Physics*, 15(15), 8889–8973.
- Movilidad y Agenda Urbana. Gobierno de España. http://www.puertos.es/es-es/estadisticas/Paginas/estadistica_mensual.aspx
- Nakada L.Y.K., and Urban C. COVID-19 pandemic: Impacts on the air quality during the partial lockdown in São Paulo state, Brazil. *Science of The Total Environment* 730, 2020, 139087. <https://doi.org/10.1016/j.scitotenv.2020.139087>
- Petetin, H., Bowdalo, L., Soret, A., Guevara, M., Jorba, O., Serradell, K., and Pérez García-Pando, C.: Meteorology-normalized impact of COVID-19 lockdown upon NO₂ pollution in Spain, *Atmos. Chem. Phys.*, 20, 11119–11141, 2020. <https://doi.org/10.5194/acp-20-11119-2020>
- Pio, C.A., and R.M. Harrison. 1987. The equilibrium of ammonium-chloride aerosol with gaseous hydrochloric-acid and ammonia under tropospheric conditions. *Atmos. Environ.* 21(5):1243–46. doi:10.1016/0004-6981(87)90253-8
- Presidencia del Gobierno, 2020. La Moncloa. Mapa de transición a la nueva normalidad. <https://www.lamoncloa.gob.es/covid-19/Paginas/mapa-fases-desescalada.aspx> (accesed 29/10/2020)
- Puertos del Estado, 2020. Autoridad Portuaria: Estadísticas Tráfico. Ministerio de Transportes, Querol, X., Alastuey, A., Gangoiti, G., Perez, N., Lee, H. K., Eun, H. R., Park, Y., Mantilla, E., Escudero, M., Titos, G., Alonso, L., Temime-Roussel, B., Marchand, N., Moreta, J. R., Revuelta, M. A., Salvador, P., Artíñano, B., Dos Santos, S. G., Anguas, M., Notario, A., Saiz-Lopez, A., Harrison, R. M., Millán, M. and Ahn, K. H., 2018. Phenomenology of summer

- ozone episodes over the Madrid Metropolitan Area, central Spain. *Atmospheric Chemistry and Physics*, 18, 9, 6511–6533.
- Querol, X., Alastuey, A., Reche, C., Orío, A., Pallares, M., Reina, F., Dieguez, J. J., Mantilla, E., Escudero, M., Alonso, L., Gangoiti, G. and Millán, M., 2016. On the origin of the highest ozone episodes in Spain', *Science of the Total Environment*. 572, 379–389.
- Querol, X., Gangoiti, G., Mantilla, E., Alastuey, A., Minguillón, M. C., Amato, F., Reche, C., Viana, M., Moreno, T., Karanasiou, A., Rivas, I., Pérez, N., Ripoll, A., Brines, M., Ealo, M., Pandolfi, M., Lee, H. K., Eun, H. R., Park, Y. H., Escudero, M., Beddows, D., Harrison, R. M., Bertrand, A., Marchand, N., Lyasota, A., Codina, B., Olid, M., Udina, M., Jiménez-Esteve, B., Jiménez-Esteve, B. B., Alonso, L., Millán, M. and Ahn, K. H., 2017. Phenomenology of high-ozone episodes in NE Spain, *Atmospheric Chemistry and Physics* 17, 4 2817–2838.
- Querol, X., Pérez, N., Reche, C., Ealo, M., Ripoll, A., Tur, J., Pandolfi, M., Pey, J., Salvador, P., Moreno, T. and Alastuey, A., 2019. African dust and air quality over Spain: Is it only dust that matters? *Science of the Total Environment* 686, 737–752.
- Reche C., Viana M., Karanasiou A., Cusack M., Alastuey A., Artíñano B., Revuelta M.A., López-Mahía P., Blanco-Heras G., Rodríguez S., Sánchez de la Campa A.M., Fernández-Camacho R., González-Castanedo Y., Mantilla E., Tang Y.S., Querol X. Urban NH₃ levels and sources in six major Spanish cities. *Chemosphere*, 119, 769-777. doi: 10.1016/j.chemosphere.2014.07.097.
- Saiz-Lopez A., Borge R., Notario A., Adame J. A., de la Paz D., Querol X., Artíñano B., Gómez-Moreno F. J., Cuevas C. A., 2017. Unexpected increase in the oxidation capacity of the urban atmosphere of Madrid, Spain. *Scientific Reports*, 7, 45956, DOI: 10.1038/srep45956
- Sicard P., De Marco A., Agathokleous E., Meng Z., Xu X., Paoletti E., Diéguez Rodríguez J.J., Calatayud V. Amplified ozone pollution in cities during the COVID-19 lockdown. *Science of The Total Environment*, 735, 2020, 133542.
- Silver B., He X., Arnold S.R., Spracklen D.V., The impact of COVID-19 control measures on air quality in China. *Environment Research Letters* 15, 2020, 084021.
- Suarez-Bertoa R. Zardini AA., Astorga C., 2014. Ammonia exhaust emissions from spark ignition vehicles over the New European Driving Cycle. *Atmospheric Environment* 97, 43-53.
- Tobías, A., Carnerero, C., Reche, C., Massagué, J., Via, M., Minguillón, M. C., Alastuey, A., and Querol, X.: Changes in air quality during the lockdown in Barcelona (Spain) one month into the SARS-CoV-2 epidemic, *Sci. Total Environ.*, 726, 138540, <https://doi.org/10.1016/j.scitotenv.2020.138540>, 2020
- UPM, 2017. Universidad Politécnica de Madrid. Estudio para la cuantificación de la Contribución de fuentes a los niveles de calidad del aire en el municipio de Madrid <https://www.madrid.es/UnidadesDescentralizadas/UDCMovilidadTransportes/AreaCentral/ficheros/Ayuntamiento%20Madrid%20Contribucion%20Fuentes%20UPM.pdf>
- Van Damme M., Clarisse L., Whitburn S., Hadji-Lazaro J., Hurtmans D., Clerbaux C., Coheur P.F., 2018. Industrial and agricultural ammonia point sources exposed. *Nature* volume 564, pages99–103.
- Van Geffen, J., Eskes, H. J., Boersma, K. F., Maasakkers, J. D. & Veefkind, J. P. (2019). TROPOMI ATBD of the total and tropospheric NO₂ data products. Royal Netherlands Meteorological Institute, #S5P-KNMI-L2-0005-RP, issue 1.4.0, 6 February 2019
- Veefkind, J. P., Aben, I., McMullan, K., Förster, H., deVries, J., Otter, G., Claas, J., Eskes, H. J., De Haan, J. F., Kleipool, Q., & Van Weele, M. (2012). TROPOMI on the ESA Sentinel-5

Precursor: A GMES mission for global observations of the atmospheric composition for climate, air quality and ozone layer applications. *Remote Sensing of Environment*, 120, 70–83. <https://doi.org/10.1016/j.rse.2011.09.027>

Zhao Y., Zhang K., Xu X., Shen H., Zhu X., Zhang Y., Hu Y., Shen G., Substantial Changes in Nitrogen Dioxide and Ozone after Excluding Meteorological Impacts during the COVID-19 Outbreak in Mainland China. *Environmental Sciences and Technology Lett.* 2020, 7, 402–408.

Journal Pre-proof

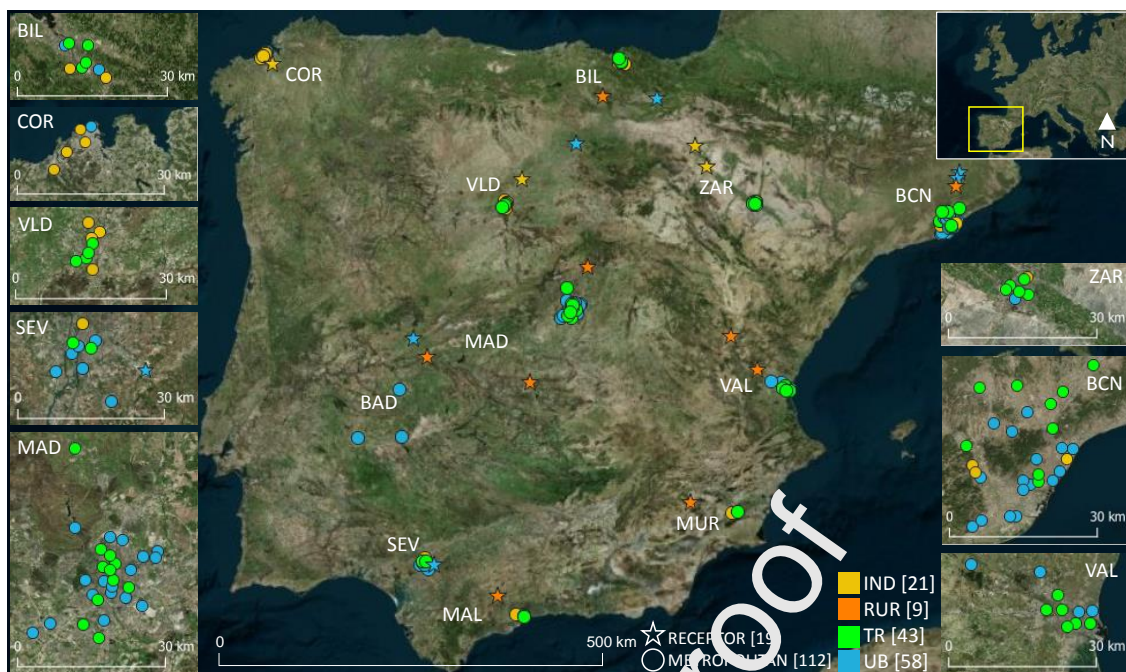


Figure 1. Area of study with 131 air quality sites across 11 metropolitan areas, Madrid (MAD), Barcelona (BCN), Valencia (VAL), Sevilla (SEV), Málaga (MAL), Bilbao (BIL), Zaragoza (ZAR), Murcia (MUR), Coruña (COR), Valladolid (VLD) and Badajoz (BAD). Circles depict metropolitan AQ sites and stars the receptor ones. Color classification according to the AQ type, industrial (IND), rural (RUR), traffic (TR) and urban background (UB).

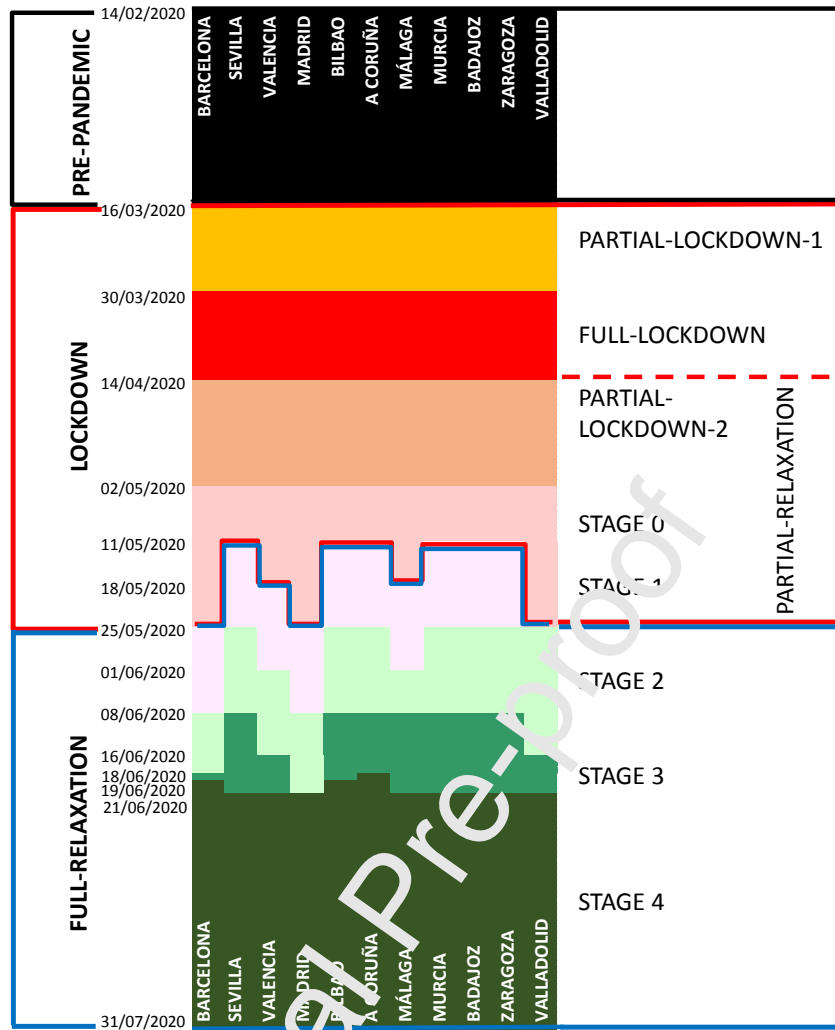


Figure 2. Periods of the reference pre-pandemic, lockdown and full-relaxation associated to the COVID19 confinement stages for the different studied cities according Presidencia del Gobierno (2020).

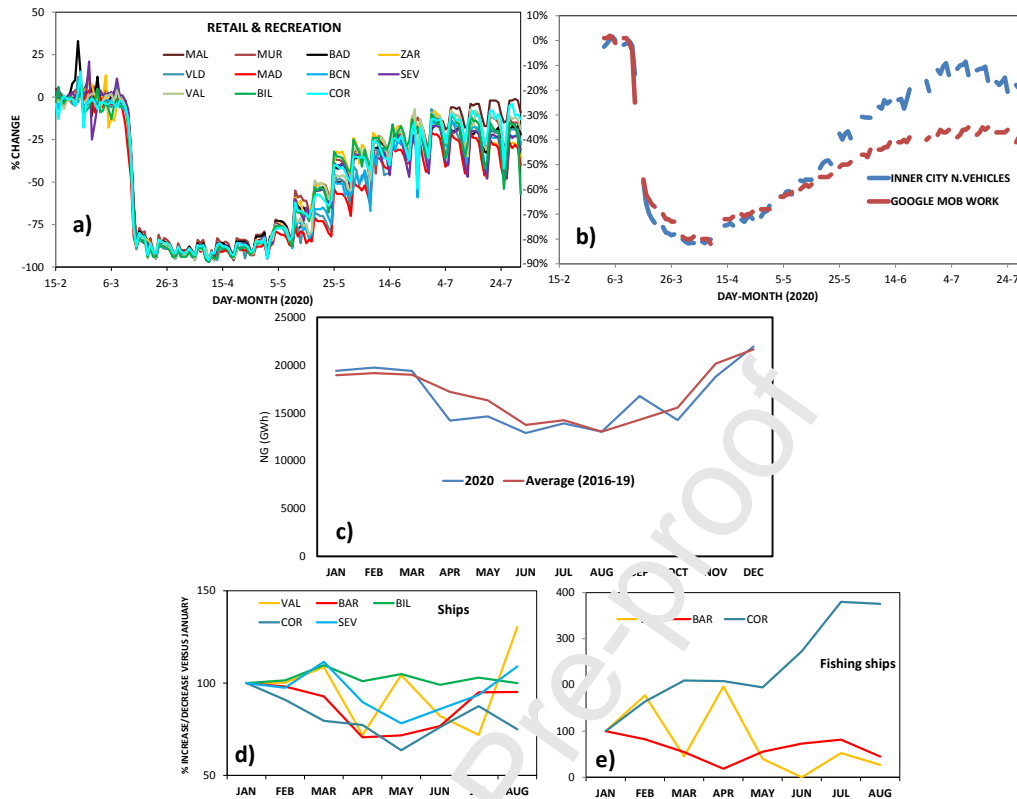


Figure 3. a) Human mobility changes (% Google LLC, 2020) from average baseline (calculated with data from 03/01 to 06/02/2020) in Málaga (MAL), Murcia (MUR), Badajoz (BAD), Zaragoza (ZAR), Valladolid (VLD), Madrid (MAD), Barcelona (BCN), Sevilla (SEV), Valencia (VAL), Bilbao (BIL) and A Coruña (COR) (Spain), before, during and after the lockdown imposed by COVID-19. b) Comparison of the relative variation of the week day circulating vehicles (provided by Barcelona City Council) and the ones for work-place Google Mobility. c) Monthly natural gas consumed by the industry in Spain (excluding power generation, in GWh) in 2020 compared with 2016-2019 averages (enagas, 2021). d) Relative changes (% Puertos del Estado, 2020) of the monthly number of ships and e) fishing ships in harbours from the study cities.

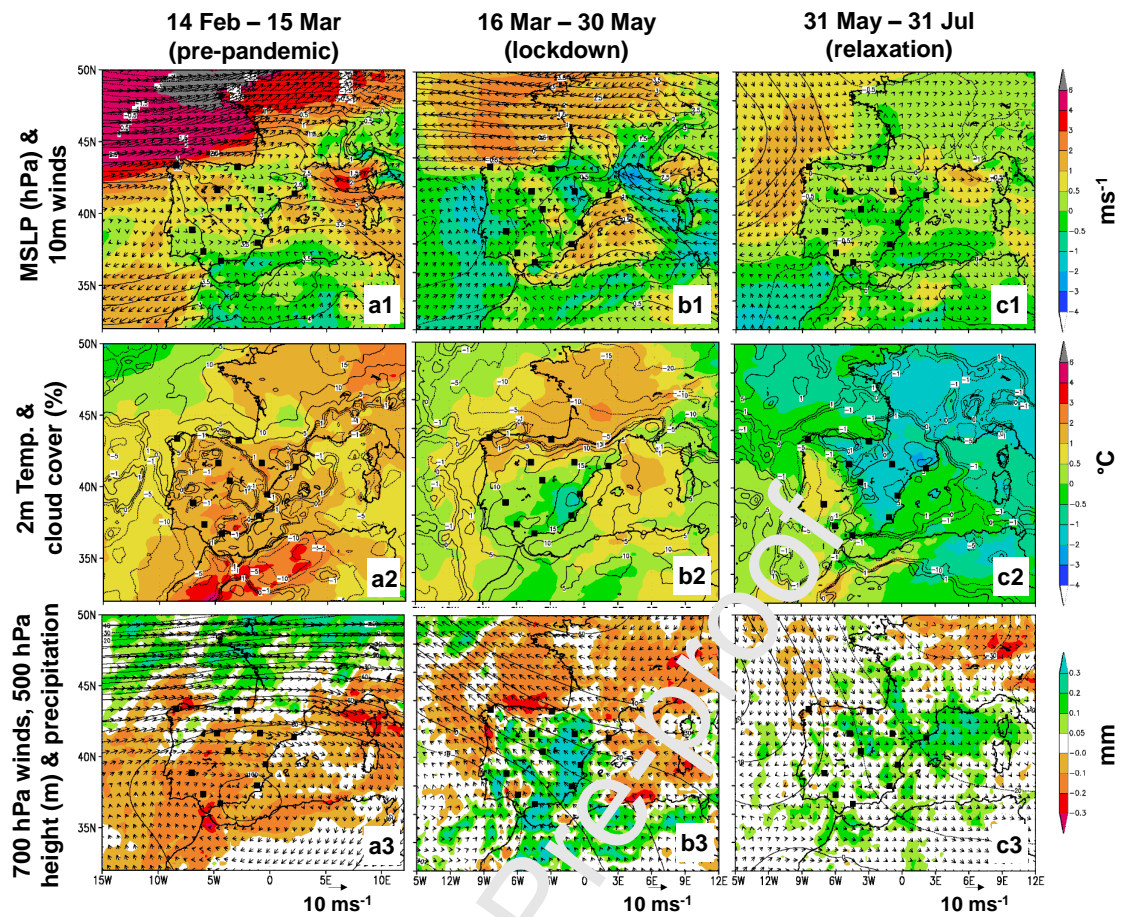


Figure 4. Anomalies of relevant meteorological parameters during pre-pandemic, lockdown and relaxation periods. Anomalies were calculated versus the 2015-2019 five-year averages of the same periods using hourly ERA5 reanalysis data.

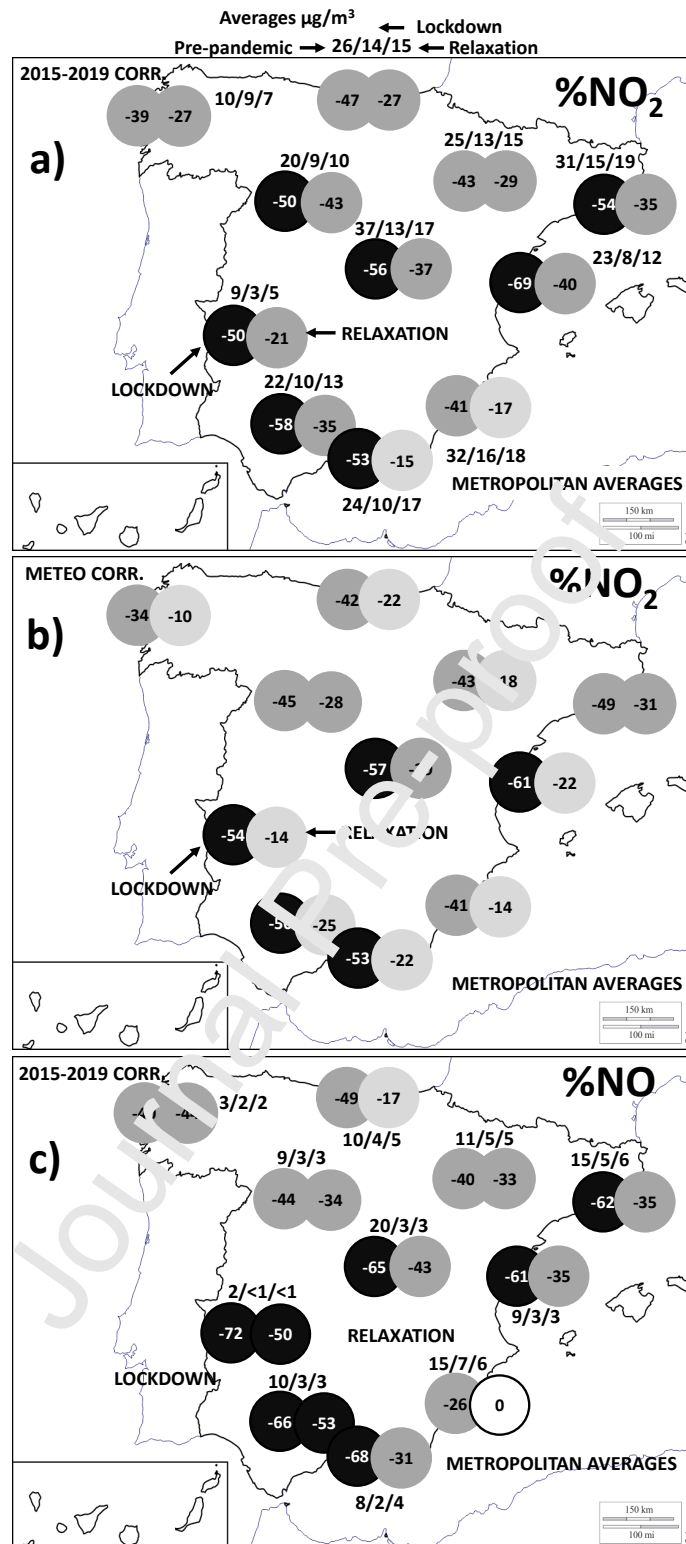


Figure 5. a) Into circles: averaged percentage change of NO₂ compared to the 2015-2019 averages; over or below circles: average concentrations (in µg/m³) during the pre-pandemic/lockdown/relaxation periods. b) Idem but circles indicate meteorology corrected reductions. c) Idem for NO concentrations and averaged percentage change of NO compared to the 2015-2019 averages.

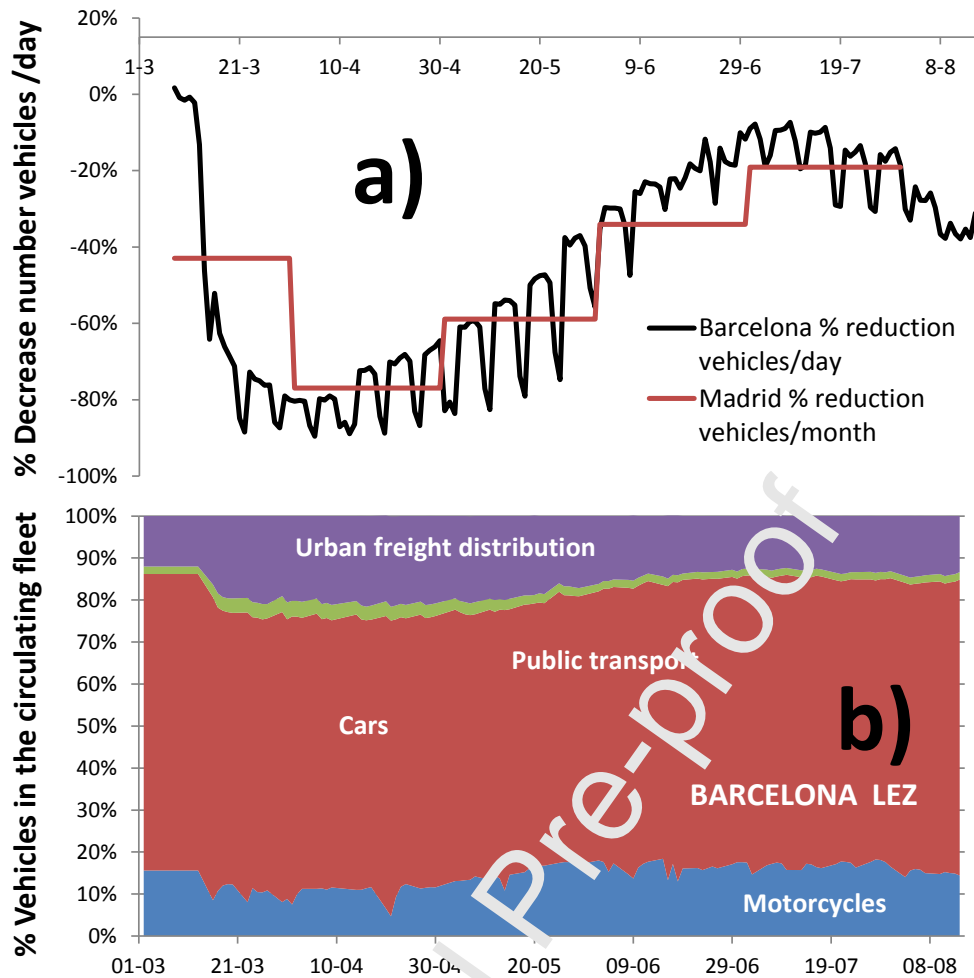


Figure 6. a) Relative decrease (compared to pre-pandemic period) of the total traffic counts per day in the city of Barcelona (daily data) and Madrid (monthly data) during the study period; b) composition of the circulating fleet in the Barcelona's Low Emission Zone. Data supplied by the Barcelona and Madrid city councils (a) and the Barcelona Metropolitan Area Administration (b).

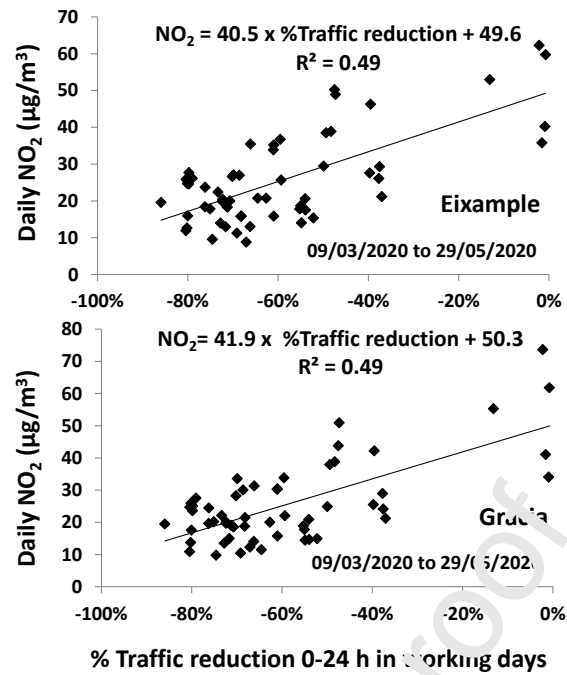


Figure 7. Cross correlation plots and regression equations for the percentage of reductions of traffic daily counts and daily NO₂ ambient concentrations recorded at two traffic air quality monitoring stations of Barcelona (Eixample and Gràcia) from before (09/03/2020) to the end (29/05/2020) of the lockdown.

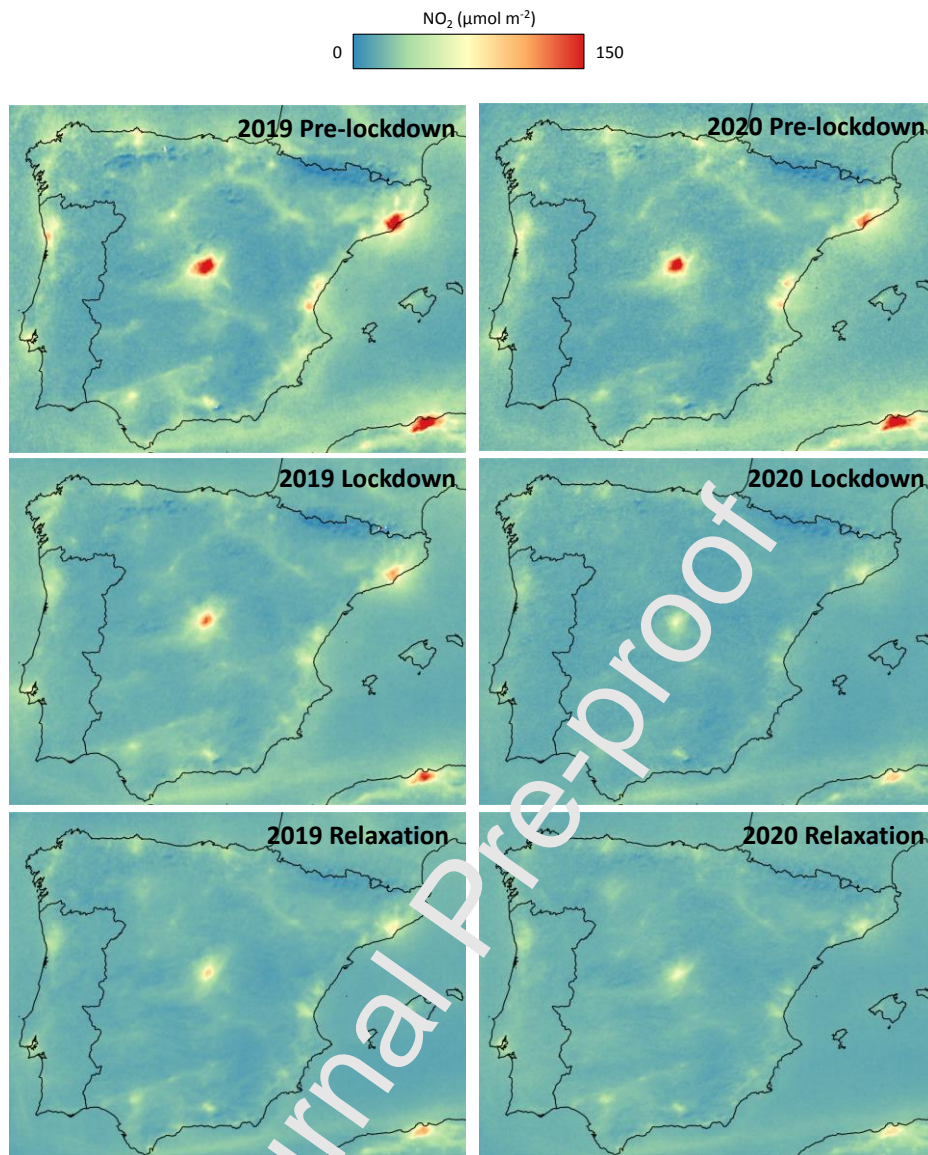


Figure 8. Maps of columnar tropospheric NO₂ levels (TROPOMI-European Space Agency, ESA) over the Iberian Peninsula for the pre-pandemic reference, the lockdown, and the relaxation periods in 2020. The maps for the same periods in 2019 are also added for comparison.

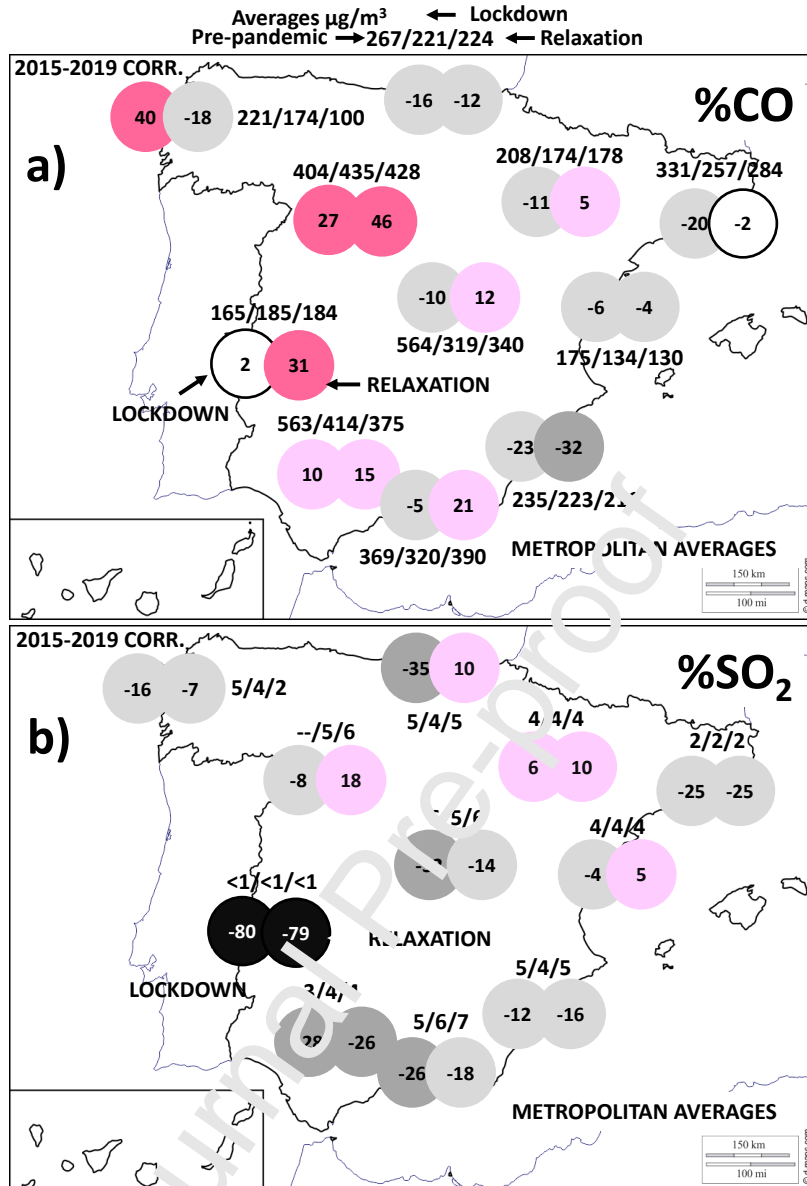


Figure 9. a) Into circles: averaged percentage change of CO compared to the 2015-2019 averages; over or below circles: mean concentrations (in $\mu\text{g}/\text{m}^3$) during pre-pandemic/lockdown/relaxation periods. b) Idem for SO_2 concentrations and averaged percentage change of SO_2 compared to the 2015-2019 averages.

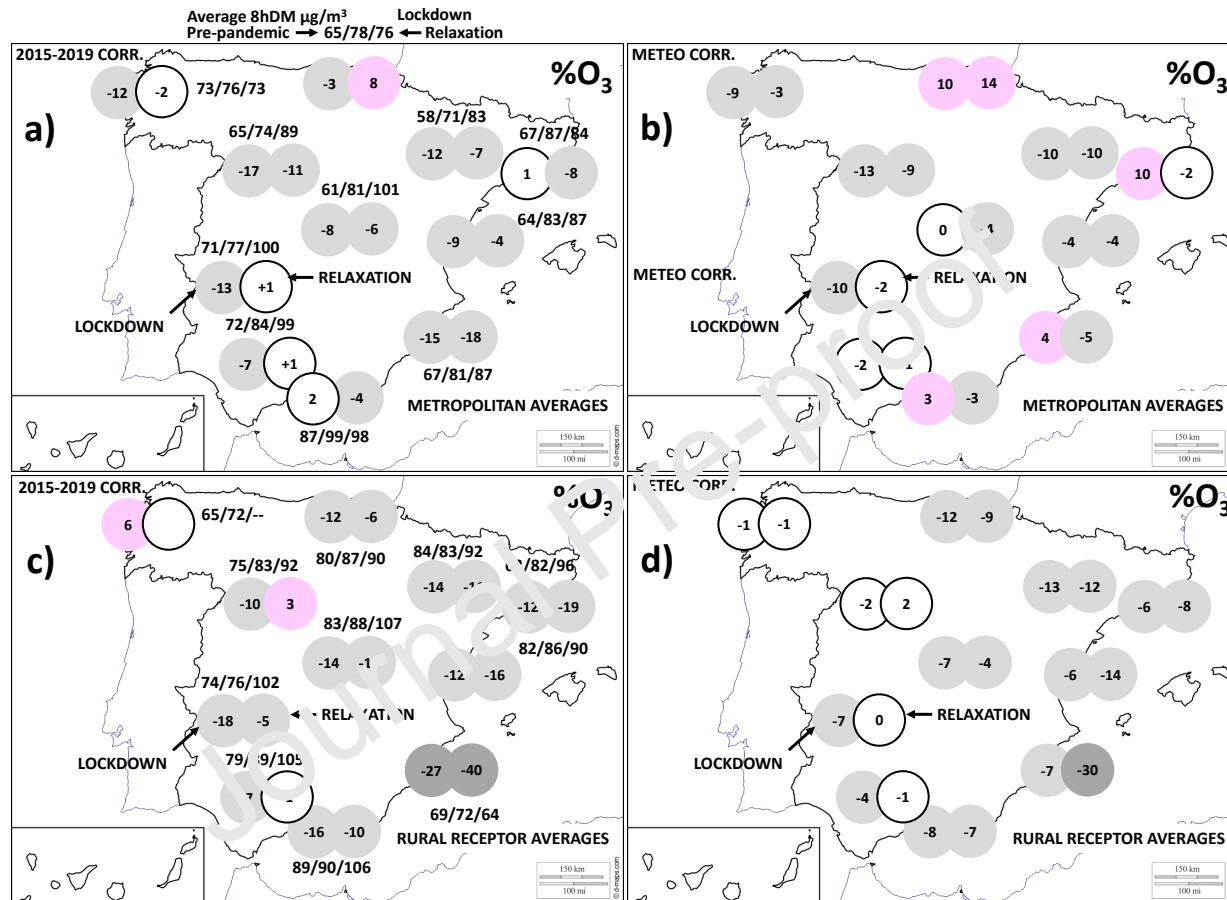


Figure 10. a) Into circles: averaged percentage change of O_3 8hDM in metropolitan areas compared to the 2015-2019 averages in metropolitan areas; over or below circles: average concentrations (in $\mu\text{g}/\text{m}^3$) during the pre-pandemic/lockdown/relaxation periods. b) Idem but circles indicate meteorology corrected reductions in metropolitan areas. c) Idem but circles indicate, for the receptor areas, the reductions compared to the 2015-2019 averages; over or below circles: average concentrations (in $\mu\text{g}/\text{m}^3$) during the pre-pandemic/lockdown/relaxation periods for the receptors. b) Idem but circles indicate meteorology corrected reductions in receptor areas.

Table 1. Main characteristics of the 11 metropolitan areas in the study, including codes used in this work to refer to each metropolitan area, number of AQ stations and other characteristics. (1) MITMA (2020), (2) DGT (2020), (3) IGN (2018). Climate classification as: Cfb: Oceanic climate; Csa: and Csb: Hot- and Warm-summer Mediterranean climates, respectively; Bsh: Warm steppe climate; Bsk: Semi-arid characteristics.

Metropolitan Area	Code	# AQ sites metrop. + receptor	Population (inhab. × 10 ⁶)(1)	Area (km ²)(1)	Population density (inhab./km ²)	# Vehicles in Province × 10 ⁶ (1)	Density / vehicles Province (#/km ²) (2)	Longitude (dec. deg.)	Latitude (dec. deg.)	Altitude (m.a.s.l)	Climate Köppen-Geiger classif.(3)
Madrid	MAD	28 + 2	6.120	2890	2118	2.084	629	-3.692	40.419	657	Csa/Bsk
Barcelona	BCN	28 + 3	5.108	3272	1561	2.744	484	2.177	41.383	13	Csa
Valencia	VAL	10 + 2	1.554	629	2463	1.722	164	-0.375	39.467	16	Csa
Sevilla	SEV	9 + 1	1.307	1529	855	1.289	92	-5.983	37.383	11	Csa
Málaga	MAL	4 + 1	0.975	817	1103	1.227	168	-4.417	36.717	8	Csa
Bilbao	BIL	8 + 2	0.902	504	1789	0.692	312	-2.953	43.262	6	Cfb
Zaragoza	ZAR	7 + 2	0.745	2295	325	0.593	34	-0.883	41.650	208	Bsk
Murcia	MUR	2 + 1	0.656	1231	533	1.106	98	-1.130	37.986	42	Bsh/Bsk
Coruña	COR	5 + 1	0.414	494	838	0.799	101	-8.383	43.367	21	Cfb
Valladolid	VLD	8 + 2	0.401	747	542	0.356	33	-4.729	41.652	690	Csb
Badajoz	BAD	3 + 2	0.158	1532	103	0.517	24	-6.975	38.880	182	Csa/Bsk

Table 2. Table 2. Average % change in 2020 levels of NO₂, NO and NH₃ in all the metropolitan areas (Metrop), urban background (UB), traffic (TR), industrial (IND) and receptor (Receptor) environments during the pre-pandemic, lockdown and the subsequent relaxation periods, compared with the respective averaged values for the same periods in 2015-2019 or after the meteorological correction (Meteo), as indicated.

2015-2019	Pre-pandemic					Lockdown					Full-relaxation				
	Metrop	UB	TR	IND	Receptor	Metrop	UB	TR	IND	Receptor	Metrop	UB	TR	IND	Receptor
NO₂															
BAD	0%	0%	-	-	-26%	-50%	-50%	-	-	-70%	-21%	-21%	-	-	-24%
BCN	-26%	-26%	-25%	-27%	-22%	-54%	-53%	-56%	-51%	-43%	-35%	-35%	-36%	-36%	-40%
BIL	-22%	-19%	-23%	-21%	-15%	-47%	-42%	-49%	-47%	-49%	-27%	-22%	-31%	-25%	-29%
COR	-32%	-39%	-	-30%	-3%	-39%	-49%	-	-3%	-27%	-27%	-27%	-	-	-
MAD	-10%	-8%	-12%	-	-17%	-56%	-55%	-58%	-	-41%	-37%	-37%	-38%	-	-10%
MAL	-7%	-6%	-15%	-6%	-	-53%	-52%	-57%	-42%	-36%	-15%	-18%	-22%	-22%	-45%
MUR	-6%	-	3%	-19%	-2%	-41%	-	-30%	-58%	-2%	-17%	-	-8%	-33%	1%
SEV	-16%	-15%	-15%	-22%	-21%	-58%	-53%	-62%	-51%	-58%	-35%	-32%	-34%	-29%	-29%
ZAR	-17%	7%	-23%	-9%	-15%	-43%	-31%	-42%	-60%	-33%	-29%	-42%	-31%	-8%	-33%
VAL	-29%	-25%	-31%	-	23%	-9%	-66%	-69%	-	-23%	-40%	-39%	-40%	-	-10%
VLD	-17%	-	-16%	-18%	-35%	-50%	-	-45%	-55%	-69%	-43%	-	-46%	-38%	-42%
AVERAGE	-17%	-15%	-18%	-19%	-15%	-51%	-51%	-52%	-50%	-41%	-30%	-30%	-32%	-27%	-26%
Meteo	Pre-pandemic					Lockdown					Full-relaxation				
NO₂	Metrop	UB	TR	IND	Receptor	Metrop	UB	TR	IND	Receptor	Metrop	UB	TR	IND	Receptor
BAD						-54%	-54%	-	-	-53%	-14%	-14%	-	-	-9%
BCN						-49%	-49%	-50%	-46%	-36%	-31%	-33%	-29%	-32%	-30%
BIL						-42%	-38%	-44%	-39%	-32%	-22%	-22%	-23%	-19%	-13%
COR						-34%	-46%	-	-31%	-37%	-10%	-15%	-	-8%	14%
MAD						-57%	-56%	-59%	-	-33%	-29%	-29%	-28%	-	16%
MAL						-53%	-57%	-57%	-41%	-65%	-22%	-28%	-20%	-13%	-50%
MUR						-41%	-	-30%	-52%	-10%	-14%	-	-5%	-22%	2%
SEV						-50%	-48%	-58%	-44%	-53%	-25%	-21%	-33%	-28%	-25%

Journal Pre-proof															
ZAR						-43%	-48%	-36%	-69%	-27%	-18%	-43%	-10%	-30%	-24%
VAL						-61%	-57%	-62%	-	-39%	-22%	-16%	-26%	-	-19%
VLD						-45%	-	-43%	-46%	-60%	-28%	-	-37%	-19%	-49%
AVERAGE						-48%	-50%	-49%	-46%	-40%	-21%	-24%	-24%	-21%	-17%
2015-2019	Pre-pandemic					Lockdown					Full-relaxation				
NO	Metrop	UB	TR	IND	Receptor	Metrop	UB	TR	IND	Receptor	Metrop	UB	TR	IND	Receptor
BAD	-14%	-14%	-	-	-47%	-72%	-72%	-	-	0%	-50%	-50%	-	-	-69%
BCN	-34%	-35%	-33%	-34%	-18%	-62%	-60%	-64%	-57%	-9%	-35%	-34%	-38%	-27%	32%
BIL	-11%	11%	-21%	-4%	-17%	-49%	-39%	-59%	-30%	-47%	-17%	11%	-37%	8%	2%
COR	-35%	-61%	-	-25%	-14%	-40%	-54%	-	37%	-25%	-44%	-44%	-	-	-
MAD	-1%	10%	-12%	-	22%	-65%	-52%	-75%	-	13%	-43%	-29%	-53%	-	10%
MAL	-21%	-24%	-7%	-66%	-	-68%	-71%	52%	-73%	-44%	-31%	-41%	-21%	-64%	-51%
MUR	10%	-	17%	-2%	-9%	-26%	-	-12%	-53%	-12%	0%	-	16%	-33%	-19%
SEV	-19%	14%	-32%	-55%	-33%	-66%	-8%	-73%	-64%	-77%	-53%	-49%	-58%	-7%	8%
ZAR	-19%	-12%	-21%	-20%	-31%	-40%	-47%	-38%	-45%	-33%	-33%	-55%	-32%	-18%	-48%
VAL	-24%	-14%	-26%	-	-41%	-61%	-42%	-65%	-	-46%	-35%	-22%	-37%	-	-27%
VLD	-7%	-	-3%	-14%	-10%	-4%	-	-38%	-57%	47%	-34%	-	-28%	-48%	-38%
AVERAGE	-16%	-14%	-15%	-28%	-20%	-54%	-55%	-54%	-52%	-29%	-34%	-35%	-32%	-27%	-20%
2015-2019	Pre-pandemic					Lockdown					Full-relaxation				
NH₃	Metrop	UB	TR	IND	Receptor	Metrop	UB	TR	IND	Receptor	Metrop	UB	TR	IND	Receptor
VAL	19%	-	19%	-	-	-9%	-	-9%	-	-	-3%	-	-3%	-	-
BIL	-36%	-	-36%	-	-	-38%	-	-38%	-	-	-33%	-	-33%	-	-
AVERAGE	-9%	-	-9%	-	-	-24%	-	-24%	-	-	-18%	-	-18%	-	-

Table 3. Average % of change in 2020 levels of CO and SO₂ and 8hDM O₃ in all the metropolitan areas (Metrop), urban background (UB), traffic (TR), industrial (IND) and receptor (Receptor) environments during the pre-pandemic, lockdown and the subsequent relaxation periods, compared with the respective averaged values for the same periods in 2015-2019 or after the meteorological correction (Meteo), as indicated.

2015-2019	Pre-pandemic					Lockdown					Full-relaxation				
CO	Metrop	UB	TR	IND	Receptor	Metrop	UB	TR	IND	Receptor	Metrop	UB	TR	IND	Receptor
BAD	-7%	-7%	-	-	-20%	2%	2%	-	-	-56%	31%	31%	-	-	-11%
BCN	-15%	1%	-33%	-	-	-20%	1%	-43%	-	-	-2%	18%	-23%	-	-
BIL	-6%	-3%	-7%	-	-19%	-16%	-1%	-24%	-	3%	-12%	9%	-22%	-	0%
COR	65%	65%	-	-	-	40%	40%	-	-	-	-18%	-18%	-	-	-
MAD	30%	35%	27%	-	98%	-10%	-19%	-3%	-	100%	12%	8%	16%	-	123%
MAL	-7%	-20%	-	32%	-	-5%	-5%	-	-	-	21%	21%	-	-	-
MUR	-24%	-	-24%	-	-	-23%	-	-23%	-	-	-32%	-	-32%	-	-
SEV	40%	4%	176%	-	68%	10%	-7%	76%	-	82%	15%	-17%	116%	-	47%
ZAR	-12%	-8%	-12%	-12%	6%	-11%	-13%	-13%	5%	4%	5%	7%	5%	5%	13%
VAL	0%	21%	-5%	-	-	-6%	9%	-1%	-	-	-4%	-4%	-4%	-	-
VLD	-10%	-	-10%	-	-	27%	-	2%	-	-	46%	-	46%	-	-
AVERAGE	5%	10%	14%	10%	27%	-1%	1%	-2%	0%	27%	6%	6%	13%	5%	35%
2015-2019	Pre-pandemic					Lockdown					Full-relaxation				
SO ₂	Metrop	UB	TR	IND	Receptor	Metrop	UB	TR	IND	Receptor	Metrop	UB	TR	IND	Receptor
BAD	-79%	-79%	-	-	52%	-30%	-80%	-	-	27%	-79%	-79%	-	-	-18%
BCN	-18%	-14%	-11%	-38%	-80%	-25%	-22%	-32%	-21%	-62%	-25%	-18%	-32%	-36%	-50%
BIL	-19%	-5%	-19%	-14%	-14%	-35%	-35%	-30%	-58%	-6%	10%	-12%	50%	-28%	-36%
COR	-21%	26%	-	-23%	-31%	-16%	15%	-	-18%	-38%	-7%	-7%	-	-	-
MAD	-32%	-11%	-42%	-	-22%	-32%	-44%	-25%	-	-11%	-14%	-36%	0%	-	67%
MAL	-39%	-48%	-	-11%	-	-26%	-40%	-	12%	-	-18%	-23%	-	-1%	-
MUR	13%	-	13%	10%	-	-12%	-	-	-12%	-	-16%	-	-17%	-15%	-
SEV	-35%	-26%	-51%	-	-39%	-28%	-14%	-55%	-	-23%	-26%	-13%	-45%	-	3%
ZAR	0%	23%	-10%	16%	-23%	6%	26%	-10%	50%	-45%	10%	51%	2%	12%	-16%
VAL	0%	-17%	10%	-	7%	-4%	-9%	-1%	-	8%	5%	-1%	7%	-	23%
VLD	-	-	-	-	-7%	-8%	-	-8%	-	-9%	18%	-	18%	-	23%
AVERAGE	-23%	-17%	-16%	-18%	-19%	-24%	-23%	-23%	-8%	-18%	-13%	-15%	-2%	-14%	-1%

2015-2019	Pre-pandemic					Lockdown					Full-relaxation				
8hDM O ₃	Metrop	UB	TR	IND	Receptor	Metrop	UB	TR	IND	Receptor	Metrop	UB	TR	IND	Receptor
BAD	-6%	-6%	-	-	-9%	-13%	-13%	-	-	-18%	1%	1%	-	-	-5%
BCN	3%	3%	4%	2%	-11%	1%	-1%	6%	2%	-12%	-8%	-9%	-6%	-2%	-19%
BIL	-7%	-6%	-	-8%	-8%	-3%	-2%	-	-5%	-12%	8%	12%	-	4%	-6%
COR	-8%	-3%	-	-12%	6%	-12%	-8%	-	-16%	6%	-2%	-2%	-	-	-
MAD	-8%	-5%	-17%	-	-7%	-8%	-7%	-12%	-	-11%	-6%	-6%	-7%	-	-10%
MAL	3%	7%	-	-7%	-7%	2%	8%	-	-11%	16%	-4%	0%	-	-12%	-10%
MUR	-16%	-	-13%	-19%	-19%	-15%	-	-11%	-19%	-27%	-18%	-	-25%	-12%	-40%
SEV	-4%	-5%	-2%	3%	-1%	-7%	-9%	6%	-7%	-7%	1%	-1%	12%	2%	-1%
ZAR	-6%	-12%	-4%	-9%	-1%	-12%	-15%	-9%	-13%	-14%	-7%	-3%	-5%	-19%	-11%
VAL	-14%	-19%	-11%	-	-4%	-9%	-17%	-5%	-	-12%	-4%	-11%	1%	-	-16%
VLD	-10%	-	-10%	-10%	-3%	-17%	-	-13%	-20%	-10%	-11%	-	-7%	-14%	3%
AVERAGE	-7%	-5%	-8%	-7%	-6%	-9%	1%	-5%	-13%	-12%	-5%	-2%	-5%	-7%	-11%
Meteo	Pre-pandemic					Lockdown					Full-relaxation				
8hDM O ₃	Metrop	UB	TR	IND	Receptor	Metrop	UB	TR	IND	Receptor	Metrop	UB	TR	IND	Receptor
BAD						-10%	-10%	-	-	-7%	-2%	-2%	-	-	0%
BCN						10%	8%	12%	9%	-6%	-2%	-3%	0%	0%	-8%
BIL						10%	10%	-	10%	-12%	14%	18%	-	9%	-9%
COR						-9%	-8%	-	-11%	-1%	-3%	-3%	-	-4%	-1%
MAD						0%	2%	-5%	-	-7%	-4%	-3%	-7%	-	-4%
MAL						3%	8%	-	-7%	-8%	-3%	-1%	-	-9%	-7%
MUR						4%	-	12%	-4%	-7%	-5%	-	-10%	-1%	-30%
SEV						-2%	-3%	8%	-5%	-4%	1%	1%	6%	-1%	-1%
ZAR						-10%	-9%	-7%	-25%	-13%	-10%	-3%	-8%	-25%	-12%
VAL						-4%	-13%	2%	-	-6%	-4%	-10%	1%	-	-14%
VLD						-13%	-	-8%	-17%	-2%	-9%	-	-7%	-10%	2%
AVERAGE						-2%	-1%	2%	-6%	-7%	-2%	-1%	-4%	-5%	-7%

Table 4. Table 4. Average % change in 2020 levels of PM10sub and PM2.5sub in all the metropolitan areas (Metrop), urban background (UB), traffic (TR), industrial (IND) and receptor (Receptor) environments during the pre-pandemic, lockdown and the subsequent relaxation periods, compared with the respective averaged values for the same periods in 2015-2019 or after the meteorological correction (Meteo), as indicated.

2015-2019	Pre-pandemic					Lockdown					Full-relaxation				
PM10 sub	Metrop	UB	TR	IND	Receptor	Metrop	UB	TR	IND	Receptor	Metrop	UB	TR	IND	Receptor
BAD	4%	4%	-	-	18%	-35%	-35%	-	-	-	-	-	-	-	-
BCN	1%	4%	-3%	-4%	-	-32%	-32%	-30%	-34%	-	-19%	-19%	-15%	-33%	-
BIL	12%	1%	23%	4%	-14%	-9%	-22%	-2%	-1%	-9%	-10%	-18%	-10%	-6%	-18%
COR	19%	60%	-	-8%	-	-12%	6%	-	21%	-	-8%	-8%	-	-	-
MAD	9%	4%	13%	-	26%	-31%	-21%	18%	-	-3%	-25%	-29%	-19%	-	-24%
MAL	-	-	-	-	-	-	-	-	-	-	-	-	-	-	-
MUR	28%	-	-	28%	23%	0%	-	-	0%	-7%	5%	-	3%	6%	-6%
SEV	-20%	-20%	-	-	-	-43%	-43%	-	-	-	-22%	-22%	-	-	-
ZAR	-26%	-12%	-32%	-	-1%	-47%	-29%	-53%	-	-10%	-38%	-18%	-47%	-	-11%
VAL	25%	2%	33%	-	98%	-32%	-18%	-38%	-	39%	3%	-13%	10%	-	40%
VLD	54%	-	54%	-	52%	-8%	-	-6%	-13%	-2%	47%	-	53%	32%	-33%
AVERAGE	12%	-7%	17%	2%	40%	-27%	-31%	-31%	-7%	3%	-5%	-21%	0%	19%	-7%
2015-2019	Pre-pandemic					Lockdown					Full-relaxation				
PM2.5 sub	Metrop	UB	TR	IND	Receptor	Metrop	UB	TR	IND	Receptor	Metrop	UB	TR	IND	Receptor
BCN	16%	2%	29%	-	-	-19%	-20%	-18%	-	-	-21%	-20%	-21%	-	-
BIL	6%	1%	10%	-	-4%	3%	6%	-1%	-	18%	-8%	1%	-18%	-	-14%
COR	-11%	14%	-	-32%	-25%	-25%	-14%	-	-32%	-28%	-7%	-7%	-	-	-
MAD	7%	13%	3%	-	21%	-10%	-5%	-13%	-	-3%	-13%	-17%	-8%	-	-16%
ZAR	-3%	-3%	-	-	-	-3%	-3%	-	-	-	2%	2%	-	-	-
VAL	25%	18%	27%	-	44%	-22%	-3%	-27%	-	39%	-8%	-10%	-8%	-	-8%

VLD	7%	-	13%	-13%	-43%	-11%	-	-13%	0%	-17%	7%	-	4%	17%	-28%
AVERAGE	7%	8%	16%	-22%	-1%	-13%	-7%	-15%	-16%	2%	-7%	-9%	-10%	17%	-16%
Meteo	Pre-pandemic					Lockdown					Full-relaxation				
PM2.5 sub	Metrop	UB	TR	IND	Receptor	Metrop	UB	TR	IND	Receptor	Metrop	UB	TR	IND	Receptor
BCN						-28%	-28%	-28%	-	-	-27%	-24%	-30%	-	-
BIL						3%	7%	-2%	-	6%	2%	13%	-9%	-	-9%
COR						-31%	-29%	-	-31%	-20%	-37%	-37%	-	-	-
MAD						-10%	-2%	-15%	-	3%	-4%	-9%	2%	-	-11%
ZAR						0%	0%	-	-	-	25%	25%	-	-	-
VAL						-39%	-15%	-47%	-	-10%	-15%	-7%	-17%	-	-21%
VLD						-1%	-	-5%	0%	18%	17%	-	17%	17%	7%
AVERAGE						-15%	-11%	-15%	-13%	-2%	-5%	-7%	-7%	17%	-8%

CRedit Authors Statement

- Xavier Querol: Conceptualization; Data curation; Formal analysis; Methodology; Supervision; Main writing - original draft.
- Jordi Massagué: Data curation; Formal analysis; Methodology; Software Validation; Visualization; Writing - review & editing.
- Gotzon Gangoiti: Conceptualization; Data curation; Formal analysis; Methodology; Supervision; Writing - review & editing.
- Miguel Escudero: Conceptualization; Data curation; Formal analysis; Methodology; Supervision; Writing - review & editing.
- Victor Vázquez: Conceptualization; Data curation; Formal analysis; Methodology; Supervision; Writing - review & editing.
- Hervé Petetin: Conceptualization; Formal analysis; Methodology; Supervision; Writing - review & editing.
- Carlos Pérez: Conceptualization; Formal analysis; Methodology; Supervision; Writing - review & editing.
- Andrés Alastuey: Conceptualization; Methodology; Writing - review & editing.
- Teresa Moreno: Conceptualization; Methodology; Writing - review & editing.
- Enrique Mantilla: Conceptualization; Methodology; Writing - review & editing.
- José Jaime Duéguez: Conceptualization; Methodology; Writing - review & editing.
- Eliseo Monfort: Conceptualization; Methodology; Writing - review & editing.
- Oriol Jorba: Conceptualization; Methodology; Writing - review & editing.
- Jesús de la Rosa: Conceptualization; Methodology; Writing - review & editing.
- Alberto Campos: Conceptualization; Data curation; Methodology; Resources; Supervision; Visualization; Writing - review & editing.
- Marta Muñoz: Conceptualization; Data curation; Methodology; Resources; Supervision; Visualization; Writing - review & editing.
- Silvia Monge: Conceptualization; Data curation; Methodology; Resources; Supervision; Visualization; Writing - review & editing.
- María Hervás: Conceptualization; Data curation; Methodology; Resources; Supervision; Visualization; Writing - review & editing.
- Rebeca Javato: Conceptualization; Data curation; Methodology; Resources; Supervision; Visualization; Writing - review & editing.
- María J. Cornide: Conceptualization; Data curation; Methodology; Resources; Supervision; Visualization; Writing - review & editing.

Declaration of interests

The authors declare that they have no known competing financial interests or personal relationships that could have appeared to influence the work reported in this paper.

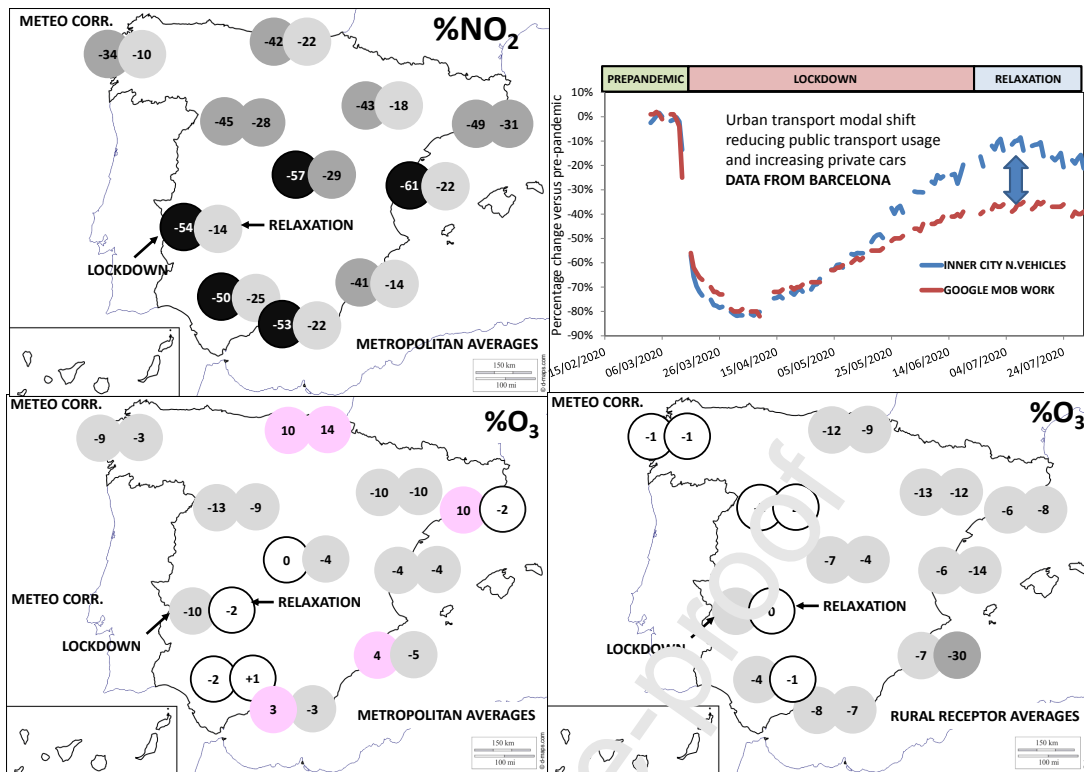
The authors declare the following financial interests/personal relationships which may be considered as potential competing interests:

All authors declare that we do not have conflicts of interest with the work done, that we do not have financial support and have personal relationships with other people or organizations that could inappropriately bias the work done.

Signed by ten corresponding author (Xavier Querol) on behalf of all authors, in Barcelona (Spain) on 2021/02/04



Graphical abstract



Highlights

COVID 19 lockdowns effects on air quality of Spain: lesson on how continuing abating pollution

We a need to recover the massive use of public transport reduced because the fear to become infected

Marked NO₂ decrease, low-than expected for PM because high NH₃ emissions in specific areas

Clear impact of domestic and agricultural biomass burning on PM and CO.

Different responses of urban O₃ in cities but generalised decrease in rural receptors.

Journal Pre-proof